MASTERARBEIT | MASTER'S THESIS

Titel | Title

Interdisciplinary application of ferromagnetic features on supply chain networks

verfasst von | submitted by

Sophia Katharina Baum B.Sc.

angestrebter akademischer Grad | in partial fulfilment of the requirements for the degree of

Master of Science (MSc)

Wien | Vienna, 2024

Studienkennzahl lt. Studienblatt | Degree programme code as it appears on the student record sheet:	UA 066 876
Studienrichtung lt. Studienblatt | Degree programme as it appears on the student record sheet:	Masterstudium Physics
Betreut von | Supervisor:	Assoc.Prof. Priv.-Doz. Mag. Dr. Peter Klimek

Acknowledgements

First and foremost, I would like to express my deepest gratitude to Stefan Thurner and Peter Klimek for the opportunity to join their research group and work on this project.

I am especially thankful to my supervisor, Peter Klimek, for his encouragement and insightful feedback throughout the course of this work. His guidance has been invaluable every step of the way.

I would also like to extend my heartfelt thanks to Moritz Laber for providing access to the static shock propagation model and for his valuable input at various stages of this research.

I am deeply grateful to Martin Bruckner for sharing an extended, unpublished version of the FABIO model, which significantly enhanced the data foundation for this project.

It has been a pleasure to collaborate with Moritz Laber, Peter Klimek, Liuhuaying Yang, and Stefan Thurner on a policy brief regarding the impact of the Indian rice embargo. I am even more excited about the perspective paper we co-authored, alongside Martin Bruckner, on the topic.

I would also like to thank the members of the Economics and Finance group at the Complexity Science Hub for the enriching discussions, their patience in answering my questions, and their generosity in sharing both literature and knowledge. Their support and insights have been an indispensable part of this process, with each conversation serving as a source of motivation.

Lastly, I am truly grateful to everyone at the Complexity Science Hub for fostering an inspiring and collaborative environment, which made working on this thesis such a memorable experience.

Abstract

The field of complex systems draws heavily on physics, which aims to make precise predictions based on experimental observations of matter and its interactions. The use of concepts and theories borrowed from physics to understand the properties and behaviour of complex networks or systems has experienced a remarkable surge, covering a wide range of applications. Trade and production relationships create a complex global supply network between countries that can be modelled using methods from physics. Here we take inspiration from hysteresis, a versatile concept derived from ferromagnetism, to model a shock to food supply chains and the subsequent compensatory behaviour. In our global food production and trade network, microscopic entities representing country-product combinations are assigned a trade and production function with node-specific parameters that inherently determine the value of that node. When a shock representing the exogenous variable is introduced, it iterates through the production and trade function to other nodes, resulting in a reduction in available commodities. Complex systems, such as the supply network we study, are adaptive, allowing entities to adjust their interactions. The mechanism behind the adaptation rules is inspired by the voter model, but fully determined in detail by global supply chain data. Using multi-regional input-output and supply-use tables for the agricultural sectors over 35 years and a model for the propagation of food supply shocks, we derive country- and product-specific adaptation rules. We apply the extended model with these adaptation capabilities to two isolated shock scenarios inspired by recent events involving Indian rice and Ukrainian wheat. We further explore the superposition of shocks and the non-linear effects on losses in the food network. By allowing for compensatory efforts in response to shocks, we offer an improved understanding of the complex systemic risks inherent in global food trade and production can inform the development of more resilient supply chains.

Zusammenfassung

Der Bereich komplexer Systeme stützt sich stark auf Physik, deren Ziel es ist, auf der Grundlage experimenteller Beobachtungen der Materie und ihrer Wechselwirkungen präzise Vorhersagen zu treffen. Die Verwendung von Konzepten und Theorien aus der Physik zum Verständnis der Eigenschaften und des Verhaltens komplexer Netze oder Systeme hat bereits einen bemerkenswerten Aufschwung erlebt und deckt ein breites Spektrum von Anwendungen ab. Handels- und Produktionsbeziehungen schaffen ebenso ein komplexes globales Versorgungsnetz zwischen Ländern, das mit Methoden aus der Physik modelliert werden kann. Hier lassen wir uns von Hysterese, einem vielseitigen Konzept aus dem Ferromagnetismus, inspirieren, um einen Schock in der Lebensmittelversorgungskette und das darauf folgende Ausgleichsverhalten zu modellieren. In unserem globalen Lebensmittelproduktions- und -handelsnetz wird mikroskopischen Einheiten, die Länder-Produkt-Kombinationen darstellen, eine Handels- und Produktionsfunktion mit knotenspezifischen Parametern zugewiesen, die den Wert dieses Knotens bestimmen. Wenn ein Schock, der die exogene Variable darstellt, eingeführt wird, wandert er durch die Produktions- und Handelsfunktion zu anderen Knoten, was zu einer Verringerung der verfügbaren Waren führt. Komplexe Systeme, wie das von uns untersuchte Versorgungsnetz, sind anpassungsfähig und ermöglichen es den Akteuren, ihre Interaktionen zu adaptieren. Der Mechanismus, der hinter unseren Anpassungsregeln steht, ist vom Voter-Modell inspiriert, wird aber im Detail durch Daten globaler Lieferkettendaten bestimmt. Anhand von multiregionalen Input-Output- und Supply-Use-Tabellen für den Agrarsektor aus 35 Jahre und einem Modell für die Ausbreitung von Schocks bei der Nahrungsmittelversorgung leiten wir länder- und produktspezifische Anpassungsregeln ab. Wir wenden das erweiterte Modell mit diesen Anpassungsmöglichkeiten auf zwei isolierte Schockszenarien an, die von den jüngsten Ereignissen, betreffend indischen Reis und ukrainischen Weizen, inspiriert sind. Außerdem untersuchen wir die Überlagerung von Schocks und die nichtlinearen Auswirkungen auf Verluste im Nahrungsmittelnetz. Indem wir kompensatorische Maßnahmen als Reaktion auf Schocks berücksichtigen, bieten wir ein besseres Verständnis der komplexen systemischen Risiken, die dem globalen Lebensmittelhandel und der Produktion innewohnen, und können die Entwicklung widerstandsfähigerer Lieferketten unterstützen.

Contents

1 Introduction

The field of complex systems draws heavily on physics, a discipline that focuses on making precise predictions based on experimental observations of matter and its interactions. While well-designed experiments should yield reliable results, the concept of predictability in physics has evolved significantly over the centuries. Initially, classical mechanics said that predictions should be exact given certain initial conditions. Statistical mechanics, however, introduced a paradigm shift, suggesting that predictions about large collectives could only apply to ensembles of microscopic entities rather than individual ones. Quantum mechanics further complicated this notion with its inherent indeterminacy, where predictions again became possible only at the collective level. In the realm of complex systems, uncertainty characterises both the components and the interactions, which can be time-dependent, non-linear and stochastic. Making predictions about such systems is possible, but requires computational and data-driven approaches. Nonlinear dynamics, which emphasises sensitivity to initial conditions, plays a crucial role in understanding these systems. In summary, although the concept of predictability has evolved, it remains essential for solving complex systems. Through empirical observation, computational analysis and nonlinear dynamics, we continue to advance our understanding of their emergent behaviour [1].

The use of physics-inspired concepts and theories to understand the properties and behaviour of complex networks or systems has experienced a remarkable surge since the second half of the 20^{th} century. This trend is evidenced by the exponential growth of publications in the field of network science, covering a wide range of applications. This surge reached a preliminary peak in 2021 when Syukuro Manabe, Klaus Hasselmann and Giorgio Parisi were awarded the Nobel Prize in Physics. Their award was attributed to their groundbreaking contributions to our understanding of complex physical systems [2]. While Manabe and Hasselmann applied complex systems methods to the study of the Earth's climate, these methods are versatile and therefore applicable to many different fields of research. Some of the most influential papers in complex systems have used them to study topics in biology such as the stability of randomly constructed genetic networks [3] and adaptive evolution [4]. In epidemiology, these methods can be used to analyse how airport transport networks are related to the spread of global epidemics [5]. In urban studies they have been used to explore scaling relationships in urban areas [6], and in finance and economics they have been instrumental in developing models of economic complexity. Such models relate the diversification of a country's economy to the structure of trade networks [7] and can provide predictions for economic growth [8]. In addition, in finance, models such as DebtRank [9] provide a measure of systemic risk in the financial sector based on an interbank leverage network.

Trade and production relations create a complex global network between countries [10, 11, 12], and the modelling of supply networks with methods from physics has been extensively studied. For example, several methods from statistical physics, such as the constrained application technique or the normal modes approach, or the application of the quasi-linear approximation of statistical physics to fluid flow models, can adequately describe the effects of real supply chains and be used to analyse and control them [13]. Purely mechanical approaches, which include basic concepts such as velocity, acceleration and force, are used to describe the evolution of supply chains in the performance space [14, 15]. It is possible to relate supply chains to transport processes of items directly to those in media. Changes in stocks of items described by material flow equations can be interpreted as discontinuous versions of the continuity equations, and changes in flows can be described by scaling relations [16].

While many papers, such as those mentioned above and [17, 18], focus primarily on changes in demand as the key driver of supply chain instability and assess adjustments in the upstream supply chain, it's equally important to examine how changes, particularly shortages, in sources of supply affect downstream supply. Shortages propagate and can develop from a sudden local reduction in available food, i.e. a shock, to potential global food security crises, often through cascading [10, 19, 20]. Shocks with such destructive potential have become more frequent in recent times [21]. Quantitative methods for assessing food security are often based on modelling food prices [22, 23, 24, 25], typically focusing on individual commodities or commodity groups and their respective trade networks [19, 26, 27, 28, 29]. However, since many commodities, especially staples such as wheat, maize, soybeans and rice, serve as inputs in production processes [30], there is increasing interest in shock propagation models that include indirect trade and production network effects [19, 31, 26, 27, 32], which means that shortages of input products can spill over into several output products along the transformation chain [31]. Traditionally, input-output (IO) models are used to capture the transformation of products into each other [33, 34]. While effective as demand-driven models for uncovering the upstream use of resources along the supply chain [30], input-output models prove less suitable for assessing supply-driven shocks [34].

To simulate shock, we draw inspiration from elements of magnetism, particularly ferromagnetism. In our global food production and trade network, microscopic entities representing country-product combinations are assigned a trade and production function with node-specific parameters that inherently determine the value of that node. This value represents the amount of the product available in the country. When a shock representing the exogenous variable is introduced, it iterates through the production and trade function to other nodes, resulting in a reduction in available goods. The impact on individual nodes can be measured and adds up to a total impact on the whole system. The amount of loss and its distribution across the system, compared to a scenario with no shock, is our macroscopic observable. The relationship between shock size and loss is not necessarily linear, similar to the relationship between magnetic field and magnetisation in ferromagnets. Neither magnetic susceptibility nor its supply chain equivalent - a shock amplification parameter - is constant, as the latter depends on the composition of the shock. Where and to which product the shock is applied will have very different effects due to the heterogeneous nature of the network.

When assessing the impact of a food supply shock on a country, the adaptive capacity of the global food trade and production network is typically neglected, with links in the food supply network treated as static [31, 19, 20], even though the system changes over time [35, 36, 28]. During the 2008 food crisis, a quarter of the 77 countries surveyed by the Food and Agriculture Organization (FAO) took measures to increase food supply [37]. Maintaining fixed food trade and production strategies for shock products in a crisis leads to exacerbated and possibly avoidable losses [38, 32, 26, 39, 29]. However, adaptation efforts to mitigate one's own losses can have spillover effects throughout the trading network due to increased competition for fewer resources [27]. A country has a wide range of options for adjusting its trade and production network. Therefore, the design of country-specific adjustment strategies usually requires detailed knowledge of the country's production capabilities, geopolitical alliances, pricing and financial capabilities [28, 29].

Complex systems, such as the supply network we are studying, are adaptive, allowing entities to adjust their interactions. This adaptability is unusual in classical physics, including magnetism, where interactions are typically fixed. In this thesis, we will allow for adaptive behaviour, as the parameters of the trade and production equations are no longer absolutely fixed, but can be adjusted when a node is severely affected by a shock, and address the challenge of developing and validating country- and product-specific adjustment rules through data-driven analysis. The mechanism behind the adjustment rules will be inspired by voter models [40], but fully determined in detail by global supply chain data. We achieve this by parameterising a response strategy model based on extensive historical food input-output and supply-use data [30] and the numerous shocks and subsequent adjustments documented therein. The modelled adjustment rules are integrated into a bipartite multi-level shock propagation model originally formulated using static recursive trade and production functions [31]. Our model explores 10^8 potential shock transmission pathways. We extend this framework by incorporating adaptive, empirically grounded and country-specific strategies for trade, production, allocation and substitution triggered by substantial losses. This allows us to simulate global outcomes of shock scenarios for specific products in different countries, and to evaluate and compare the effectiveness of different adaptation strategies across countries and products. Adaptation capabilities are local, node-specific and scaled by the severity of the shock to the affected node. The aim of this work is to determine how the effect on microscopic entities affects macroscopic parameters such as the relative loss to the system (analogous to susceptibility).

In addition, we use this framework to provide a comprehensive overview of historical food availability shocks, to explore general patterns in countries' responses to these shocks, and to identify effective, and therefore key, microscopic adjustment rules. To study the macroscopic effects, we examine two specific hypothetical scenarios inspired by recent geopolitical events: a total embargo on Indian rice [41, 42] and a disruption of Ukrainian wheat exports due to the ongoing Russian invasion [43, 44]. For both scenarios, we consider a worst-case scenario of a complete loss of production and assess the resulting impact on the global availability of the products as well as on secondary commodities. In addition, we examine the combined effects of the two shocks, as rice and wheat can act as substitutes for each other.

2 From magnetism to adaptive food supply networks

The aim of this chapter is to provide an insight into magnetism as an explanatory concept for the propagation of supply chain shocks. First, we introduce ferromagnetism and take a closer look at hysteresis, a concept rooted in magnetism but also widely used in economics. Second, we explore the application to complex systems in the form of voter models and illustrate how adaptive interactions can be integrated into the framework.

2.1 Translating effects in ferromagnetism to shock propagation on food supply networks

Magnetism encompasses a range of physical characteristics that manifest in a magnetic field. When discussing magnetism, the typical image is of the attraction and repulsion between two magnets. Phenomenologically, it is often described as involving two 'free' magnetic monopoles, although in reality, such monopoles cannot exist due to Gauss's law for magnetism [45], which states that the divergence of a magnetic field $\vec{B}$ is 0:

$$\nabla \vec{B} = 0 \quad . \tag{2.1}$$

If two monopoles, each with opposing signs, reside at the ends of a common magnet, they exert a force on each other known as the Coulomb force. The force between two magnetic poles of strength m_1 and m_2, separated by a distance r in a vacuum with permeability $\mu_0 = 4\mu \times 10^{-7}\,\frac{\mathrm{H}}{\mathrm{m}}$, is given by Coulomb's law [46]:

$$F = \frac{m_1 m_2}{4\pi\mu_0 r^2} \quad . \tag{2.2}$$

The equation's structure is reminiscent of Newton's law of universal gravity, which describes the gravitational force between two masses separated by a distance and scaled by the gravitational constant G [47]. A region of space where magnetic poles exert force is called a magnetic field. It can magnetize materials to varying degrees, depending on their characteristics. Some materials are easily attracted by a simple permanent magnet, while for others, magnetization $\vec{M}$ may only be detectable with very sensitive instruments. Permanent magnetic materials only require magnetization once and then maintain it even in the absence of any magnetic field. Quantitatively, the magnetization $\vec{M}$ indicates the density of magnetic dipole moments $\vec{m}_i$, regardless of whether they are permanent or were induced:

$$\vec{M} = \frac{\mathrm{d}\vec{m}}{\mathrm{d}V} \quad . \tag{2.3}$$

$\mathrm{d}\vec{m}$ represents the elementary magnetic moment, while $\mathrm{d}V$ denotes the volume element.

The magnetic field strength $\vec{H}$ is connected to the magnetic flux density $\vec{B}$ in the absence of any magnetic or dielectric materials by the vacuum permeability μ_0:

$$\vec{B} = \mu_0 \vec{H} \quad . \tag{2.4}$$

Both $\vec{H}$ and $\vec{B}$ are pseudo-vector fields and are commonly referred to as magnetic fields, despite describing distinct physical quantities.

In diamagnetic and paramagnetic materials, the relationship between the two types of magnetic fields and the magnetization $\vec{M}$ are typically linear:

$$\vec{B} = \mu\vec{H} \quad . \tag{2.5}$$

with the material permeability μ and

$$\vec{M} = \chi\vec{H} \quad . \tag{2.6}$$

with the magnetic susceptibility χ.

The magnetic flux density $\vec{B}$ can also be expressed as the sum of the magnetic field strength $\vec{H}$ and the magnetization $\vec{M}$ in vacuum which has to equal (2.5):

$$\vec{B} = \mu_0(\vec{M} + \vec{H}) = \mu_0(\chi\vec{H} + \vec{H}) = \mu_0(\chi + 1)\vec{H} \stackrel{!}{=} \mu\vec{H} \quad . \tag{2.7}$$

So, we can deduce this relationship between the parameters:

$$\chi = \frac{\mu}{\mu_0} - 1 \quad . \tag{2.8}$$

From equation (2.6), we know that the magnetization of a material should be directly proportional to the magnetic field. This holds true for weakly magnetic materials with low values of magnetic susceptibility (χ) and permeability (μ), such as para- or diamagnetic materials. However, for ferromagnetic materials, which exhibit very high magnetic permeability (μ), this relationship becomes more complex, and we observe hysteresis (Figure 2.1). When a magnetic field is applied to a ferromagnet, the magnetic dipoles align themselves with the external field, resulting in magnetization of the material. This magnetization persists even after the external field is removed, as the ferromagnet becomes permanently magnetized. Demagnetizing the material requires additional measures such as applying heat, another magnetic field, or a magnetic field of opposite polarity [48].

To understand the macroscopic behavior of ferromagnets, considering the spin of electrons can offer a comprehensive theory [50], summarized in the following paragraphs. Each electron, or magnetic dipole, can be assigned a spin of either up, represented as μ, or down, represented as $-\mu$. The energy of an orientation in a magnetic field is not solely determined by the external field H, but also by the orientation of the neighborhood, which is indicated by the mean absolute value of the neighboring magnetization vector field $\vec{M}$, denoted as M,

$$E = \pm\mu(H + \frac{\lambda M}{\epsilon_0 c^2}) \tag{2.9}$$

with a material-dependent parameter λ . The total magnetization at a temperature T is therefore:

$$M = N\mu \tanh(x) \quad \text{with} \tag{2.10}$$

$$x = \frac{\mu(H + \frac{\lambda M}{\epsilon_0 c^2})}{k_B T} \tag{2.11}$$

with the Boltzmann constant $k_B = 1.381 \times 10^{-23}\,\frac{\mathrm{J}}{\mathrm{K}}$, the vacuum permittivity $\epsilon_0 = 8.854 \times 10^{-12}\,\frac{\mathrm{F}}{\mathrm{m}}$, and the speed of light in vacuum $c_0 = 2.998 \times 10^8\,\frac{\mathrm{m}}{\mathrm{s}}$. The saturated magnetic moment M_{sat} indicates the maximum possible moment if all spins are aligned in the same direction:

$$M_{\mathrm{sat}} = N\mu \quad . \tag{2.12}$$

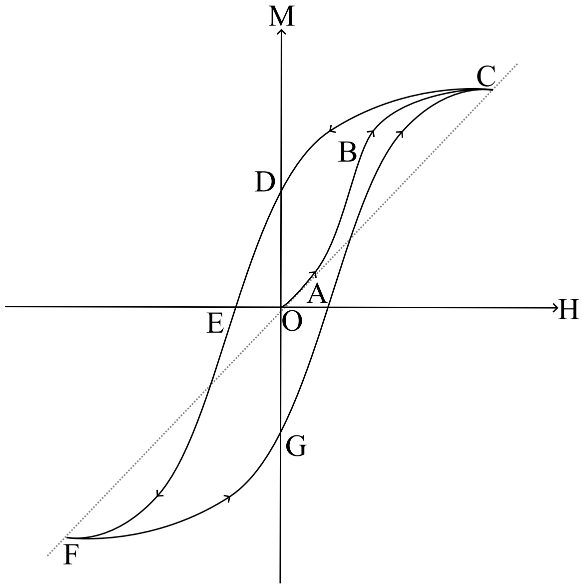

Figure 2.1: Hysteresis loop: Starting at point O where $H = M = 0$, the magnetic field is switched on ($H > 0$). The magnetization increases along the path OABC until it reaches the saturation magnetization. Upon decreasing the magnetic field, the magnetization does not follow the same path OABC in reverse, but instead follows path CDEF. The value $\overline{\mathrm{OD}}$ represents the residual magnetization, which is the magnetization that remains even when the magnetic field returns to zero. The value of $\overline{\mathrm{OE}}$ represents the coercive field, which is the magnitude of the magnetic field ($H < 0$) required for the magnetization to change sign. If the magnetic field is further increased in a negative direction, the magnetization reaches negative saturation. Upon increasing the magnetic field again, the magnetization follows path FGC. The entire path traced out by the magnetization is known as the hysteresis loop. The grey dotted line represents the hypothetical scenario where M would be directly proportional to H, which is only approximately true for ferromagnets that experience hysteresis, but usually correct for dia- or paramagnets [48, 49].

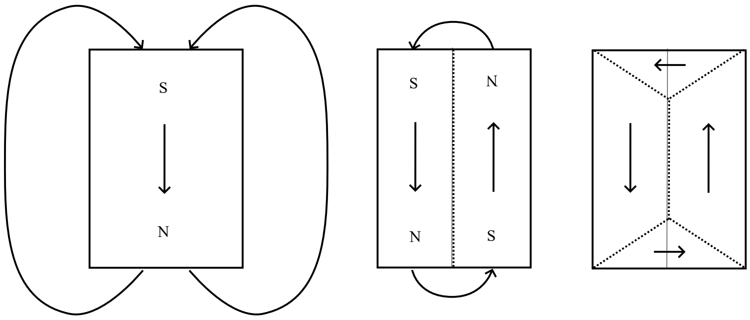

Figure 2.2: Magnetic domain evolution during magnetization: If an object spontaneously magnetizes in one direction, it would generate a large magnetic field, resulting in high magnetic field energy (left). To reduce this energy, the object can split into two domains with opposite magnetization. While this significantly reduces the size of the magnetic field, it leads to the formation of walls between the domains, which themselves result in additional energy. However, this additional energy is not as significant as the reduction in magnetic field energy (middle). Introducing triangular domains between the two opposing domains with sideways magnetization can almost completely eliminate the external magnetic field. Thanks to their triangular shape, these domains also minimize the occurrence of wall effects (right) [50].

Using that, we can derive the recursive rule

$$\frac{M}{M_{\text{sat}}} = \tanh\left(\frac{T_C}{T}\frac{M}{M_{\text{sat}}}\right)\text{with} \tag{2.13}$$

$$T_C = \frac{\mu\lambda M_{\text{sat}}}{k_B\epsilon_0 c^2} \quad . \tag{2.14}$$

This equation is particularly easy to solve for very low or very high temperatures. If T is very low, then almost all dipoles are aligned in the same direction, except perhaps for a few. Conversely, if T is very high, then the distribution of spin directions is almost random. While solutions for behavior near these limits may be obtained by deviating slightly from the fairly straightforward solution, the behavior around the Curie point T_C has never been thoroughly determined.

In reality, objects are typically not magnetized even when their temperature is well below T_C. If a material like iron were to spontaneously magnetize in one direction, it would generate a significant magnetic field. To reduce the energy associated with this field, the material could form domains with opposite magnetization. However, the interfaces between these domains would introduce additional energy for the electrons neighboring the opposite domain. Whether it is more advantageous to form multiple domains or not depends on the size of the domains. Objects larger than $\frac{1}{100}$ mm typically divide into domains. Some domains may also orient sideways to almost entirely circumvent external magnetic fields, albeit with minimal additional domain walls, as the sideways domains interact less with the others (Figure 2.2). A larger object may consist of numerous domains with varying orientations.

When a small external magnetic field is applied, the domain walls begin to move slightly, and those with favorable orientations grow larger. Since the field remains relatively small, the changes are reversible. However, for larger fields, reversibility is lost. Real-life objects often contain defects or imperfections, causing domain walls to become stuck at certain field magnitudes and suddenly move when the field increases further. This motion is not smooth, and on a microscopic scale, the steps in the hysteresis curve become visible. These sudden movements may result in energy loss, rendering a step along the magnetization curve irreversible. At very high magnetic fields, most domain walls

Table 2.1: Comparison of characteristics in magnetism and supply chain equivalents

General concept	Magnetism	Food supply chain network
Microscopic entities	Electrons	Network nodes (country $\times$ food product)
Microscopic states	Spin	Available amount
Microscopic equation of states	Energy	Trade and production function
Exogenous variable	Magnetic field strength	Supply shock
Transmission coefficient	Magnetic susceptibility	Shock propagation
Macroscopic observable	Magnetization	Impact density

have already moved beyond the defects, and the remaining ones are extremely reluctant to change their orientation. Reaching saturation magnetization, where all electrons are aligned, requires a significant additional effort, typically in the form of much higher magnetic fields. However, this final part of the magnetization occurs smoothly, as the defects causing sudden jumps have been removed earlier. When one starts to remove the magnetic field again, domains begin to realign towards their original constitution to reach the lowest energy state. Lowering the magnetic field gradually or setting it to zero only resets the domain walls to some extent right away, as they cannot overcome the material's deficiencies again without additional energy. Overcoming deficiencies is only possible in sudden jumps in a similar manner as it did when increasing the magnetic field initially. As saturation magnetization in the opposite direction is approached, the reset curve becomes smooth again as the material has now fully overcome its deficiencies again and only the reluctant remaining domains are left which need again comparably high magnetic fields to become aligned with the rest. This loop is completed by increasing the magnetic field in the original direction (Figure 2.1). The material behaves in the same manner as when applying the magnetic field for the first time.

If the curve is very flat at the height of the saturation magnetization leading to a high residual magnetization, meaning that magnetization that is left when the magnetic field has become zero, it represents a permanent magnet. It only has to be magnetized once, but now the magnetization remains relatively stable despite a missing magnetic field. Even fields that are directed in the opposite direction cannot turn the magnetization around or diminish it, as the saturated part of a permanent magnet's hysteresis loop is that flat.

Application in shock propagation in food supply chain network

Hysteresis is a phenomenon where a system tends to remain in its current state even after the factors that caused that state have been removed. The term is derived from the Greek word ὑστέρησις, meaning 'deficiency' or 'lagging behind'. Hysteresis is observed in various fields like physics, chemistry, biology, engineering, and economics, but its origins lie primarily in magnetism. James Alfred Ewing was one of the first to study hysteresis, particularly in the behavior of ferrous metals during magnetic cycles [49]. Economics, in particular, leverages this phenomenon to explain certain effects. For instance, persistently low employment rates at the end of a recession or the continuation of newly implemented policies even after the favorable conditions that prompted them have disappeared are two examples [51]. In economics, hysteresis refers to a situation where the state of the economy persists even after the original cause for that state has been removed. The impacts of hysteresis on a system are often observable following extreme events such as recessions or crashes.

Here, we investigate the adaptive behavior of countries in response to supply shocks. Table 2.1 provides an overview of how quantities from magnetism and its supply chain equivalents are related. Similar to magnetic materials, our food supply networks are comprised of a multitude of microscopic entities. In this case, each entity is represented by a country-product node. To each of those nodes, we assigned a value, indicating the available amount of the product in the country. The availability is determined by a trade and production function, which is specified by node-individual production and trade parameters. Additionally, it uses adjacent nodes' values as inputs in the function, akin to the energy equation. The energy of an electron in a magnetic material does not only depend on its own value but also on the mean magnetization of its neighborhood (2.9). The future available amount depends on its current value itself as the product can be used as input in a self-replicating production process, but other kinds of production processes that use inputs from other product nodes of the same country or trades with another country of the same product-type can also provide additional amounts. Now, we introduce the exogenous variable: a production shock. The shock forces one or multiple nodes to assume a value of zero or a value reduced by a significant share compared to what the node would have naturally assumed after evaluating the production and trade function. The absence of goods in singular nodes can result in reductions of available amounts of other entities as well, as they might be used as inputs in the production process or exported to other countries. The shock iterates through the network and can potentially affect the value of a wide range of nodes across the entire system to different extents. The closer a node is to the shocked one, the stronger the effect is felt. After the system assumes a steady state, we can observe its constitution. We observe the total leftover amount of all available products and compare it to the original amount. The overall reduction from the original to the shocked state serves as the equivalent of the macroscopic observable - the size of the shock impact, but also how it is distributed over the system. One can relate the shock size to shock impact by a transmission coefficient, in this case, a shock propagation parameter. The shocked node is likely to lose more product in total than was initially deleted by the shock. The amplification is not constant but highly dependent on the structure of the system and on the shock itself. This is akin to the case of ferromagnetism, where the purely linear relation of paramagnetism does not hold anymore. Whether the shocked product is a primary product and whether the shocked country is an active exporter of that product is highly important to the overall impact of a shock as our food supply network is highly heterogeneous.

2.2 Complex systems model inspired from magnetism - the voter model

When Ernst Ising published his attempt to describe ferromagnetism with his later after him called model as a one-dimensional lattice of interacting spins [52], he did not receive much attention. Only when Lars Onsager solved a two-dimensional square lattice 19 years later [53], it started to collect the accolades it deserves. Many model in complex systems are based on the Ising model which describes a system of binary magnetic spins, being in either spin-up or spin-down state, that is trying to minimize its Hamiltonian [54].

One of those models is the voter model [40] that initially was introduced to describe opinion dynamics, but also any kind of social interaction, e.g. cooperation, and other kinds contagion effects from the spread of information to one of diseases can be modelled [55, 56]. The aim was to capture the major characteristics of social behaviour with the introduction of only rather simple rules. Notably, the voter model is one of few in many dimensions solvable stochastic many-body systems and therefore rather popular as a benchmark, for perturbation solutions or as an extension of other spin systems such as Ising models or spin glasses [57].

In the simplest version of the voter model, we have a network N nodes and L links which is usually connected. Each node can obtain one of two states. Depending on the application, those could either be the status of being switched on or off, negative or positive spin or just the association with one two binary categories. At each time step, a random node i within the network is picked. According to a probability $p = f(x_i)$ that is dependent on the share of links to nodes of the opposing status x_i, the status is changed or kept (Figure 2.3). The original, simplistic version of the voter model sets $p = x_i$. The node selection and status update is repeated until a consensus is reached, implying that every node has the same status.

The consensus time $T(x)$ and the exit probability $E(x)$ with x representing the share of nodes

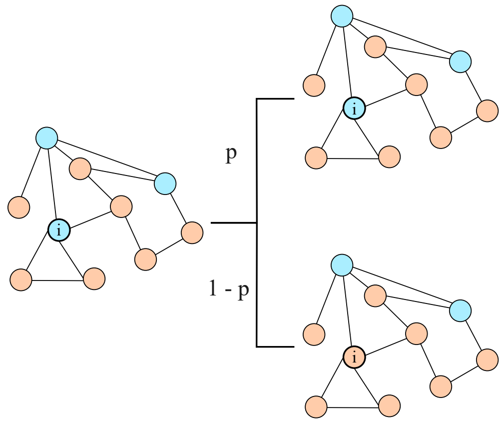

Figure 2.3: Schematic sketch on the mechanics of an easy voter model: A node i is randomly selected in a network consisting of N nodes of which each has either state *blue* or *orange*. According to some probability $p = x_i$, the node either keeps or changes its state. x_i is the share of links of node i to nodes of opposing state. This procedure is repeated until unanimity, so all nodes of the network occupy the same state, is reached.

being of either of statuses are two macroscopic observables that describes the behaviour of the system. For the notation, we will follow [55] for the rest of chapter. The probability distribution that the system displays share x at time τ is $P(x, \tau)$. The expected share $x^*(\tau)$ can therefore be calculated:

$$x^*(\tau) = \sum_x xP(x, \tau) \quad . \tag{2.15}$$

After every time step τ, the probability distribution can potentially change. We derive the probability of observing $P(x, \tau+1)$ backwards by summing up over all possible transitions from the previous state of x' which probability is described by $P(x', \tau)$ with the transition probability $\gamma(x, x')$:

$$P(x, \tau + 1) = \sum_x \gamma(x, x')P(x', \tau) \quad . \tag{2.16}$$

We want to obtain the time evolution of the probability distribution $\frac{\partial P(x,t)}{\partial t}$. First, the discrete difference is derived:

$$P(x, \tau + 1) - P(x, \tau) = \sum_{x'} \gamma(x, x')P(x', t) \quad . \tag{2.17}$$

Combing (2.15) and (2.16) yields:

$$x^*(\tau + 1) = \sum_x xP(x, \tau + 1) = \sum_x x \sum_{x'} \gamma(x, x')P(x', t) = \sum_{x'} P(x', t) \sum_x x\gamma(x, x') \quad . \tag{2.18}$$

For large N, we can assume that the step from x to x' becomes continuous as $x' + \Delta x'$ or $x' - \Delta x'$ with the respective transition probabilities $\gamma(x' + \Delta x', x')$ and $\gamma(x' + \Delta x', x')$, short as $\gamma^+(x')$ and

$\gamma^-(x')$. $x^*(\tau+1)$ becomes:

$$x^*(\tau+1) = \sum_{x'} x' P(x',\tau) + \frac{1}{N} \sum_{x'} P(x',\tau)[\gamma^+(x') - \gamma^-(x')] \tag{2.19}$$

$$= x^*(\tau) + \frac{1}{N} \sum_{x'} P(x',\tau)[\gamma^+(x') - \gamma^-(x')] \tag{2.20}$$

$$= x^*(\tau) + \frac{1}{N}[\gamma^+(x') - \gamma^-(x')] \quad . \tag{2.21}$$

The reduction in (2.21) is possible as we assume in the spirit of mean-field theory that the probability does not fluctuate locally. We obtain a recursive formula for the expectation value of the share $x^*(\tau)$. The rate of change can also be expressed with a according to the network size N rescaled time variable $t = \frac{\tau}{N}$:

$$\frac{\mathrm{d}x^*(t)}{\mathrm{d}t} = \gamma^+(x') - \gamma^-(x') \quad . \tag{2.22}$$

The rate of change for the probability distribution $\frac{\partial P(x,t)}{\partial t}$, we utilize the transition rate $\Gamma(x,x') = \frac{\gamma(x,x')}{\Delta t}$:

$$\frac{\partial P(x,t)}{\partial t} = \sum_{x'} \Gamma(x,x') P(x',\tau) - \sum_{x'} \Gamma(x',x) P(x,\tau) \quad . \tag{2.23}$$

For large enough N, where time and Δx become continuous, this can be approximated by the Fokker-Planck equation [58, 59]:

$$\frac{\partial P(x,t)}{\partial t} = -\frac{\partial}{\partial t}[V(x)P(x,t)] + \frac{1}{2}\frac{\partial^2}{\partial t^2}[D(x)P(x,t)] \quad . \tag{2.24}$$

$V(x)$ and $D(x)$ are the drift and diffusion coefficient respectively with

$$V(x) = \gamma^+(x') - \gamma^-(x') \quad \text{and} \tag{2.25}$$

$$D(x) = \frac{1}{N}[\gamma^+(x') + \gamma^-(x')] \quad . \tag{2.26}$$

Easy expressions for the transition probabilities $\gamma^+(x')$ and $\gamma^-(x')$ [60] are

$$\gamma^+(x') = (1-x)f(x) \quad \text{and} \tag{2.27}$$

$$\gamma^-(x') = xf(1-x) \quad . \tag{2.28}$$

For $f(x) = x$ as it is the case in the simple voter model, we derive $V(x) = 0$ and $D(x) = \frac{2x(1-x)}{N}$ according to (2.25) and (2.26). We can obtain the exit probability $E(x)$ by setting (2.24) to zero:

$$-\frac{\partial}{\partial t}[V(x)E(x)] + \frac{1}{2}\frac{\partial^2}{\partial t^2}[D(x)E(x)] = 0 \quad . \tag{2.29}$$

Inserting $V(x)$ and $D(x)$ results in

$$\frac{x(1-x)}{N}\frac{\partial^2}{\partial t^2}E(x) = 0 \quad . \tag{2.30}$$

$\frac{x(1-x)}{N}$ is only zero for $x \in \{0,1\}$, so $\frac{\partial^2}{\partial t^2}E(x)$ has to be zero elsewhere. Integrating twice yields the general result for $E(x)$. With the boundary conditions $E(0) = 0$ and $E(1) = 1$, we can conclude

$$E(x) = x \quad . \tag{2.31}$$

Similarly, we can obtain the consensus time $T(x)$ by setting (2.24) to minus one:

$$-\frac{\partial}{\partial t}[V(x)T(x)] + \frac{1}{2}\frac{\partial^2}{\partial t^2}[D(x)T(x)] = -1 \quad . \tag{2.32}$$

After inserting $V(x)$ and $D(x)$, we get

$$\frac{x(1-x)}{N}\frac{\partial^2}{\partial t^2}T(x) = -1 \quad . \tag{2.33}$$

By rearranging and separating the fraction, the expression becomes easily integrable:

$$\frac{\partial^2}{\partial t^2}T(x) = -\frac{N}{x(1-x)} = -N\left(\frac{1}{x} - \frac{1}{1-x}\right) \quad . \tag{2.34}$$

Integrating twice yields the general result for $T(x)$. With the boundary conditions $T(0) = 0$ and $T(1) = 0$, we can conclude

$$T(x) = -N\big(x\ln(x) + (1-x)\ln(1-x)\big) \quad . \tag{2.35}$$

The version of the voter model only represent a very uncomplicated edition as it only describes single variable, binary and single-flip procedure with the simplest possible selection probability. Allowing for multiple-flips, the choice between more than two states or even a continuous variable and instead of a single determining value a vector provides a broad variety of new models. One can also extend to function of the switch probability to the non-linear q-voter model where q neighbour instead of one are randomly picked for influencing the voter [60]:

$$p(x,q) = x^q + \epsilon\big(1 - x^q - (1-x^q)\big) \quad . \tag{2.36}$$

As the voter model originated in opinion dynamics, there have been attempts of explicitly modeling evident behaviour in opinion formation such as non-conformity which can appear either as independence or anti-conformity [55]. Other reality-inspired extension include heterogeneous, non-conserved dynamics, confident voter, stubbornness or compromise models [56].

Complex systems, such as the supply network under consideration, are adaptable and can adjust the strength or even existence of interactions between nodes [61]. This adaptability is inherently uncommon in physics, including magnetism, where the state of nodes can be uncertain, but interactions are typically fixed. Here, we will allow for adaptive behavior, and parameters of the trade and production functions are no longer entirely static but can be adjusted if a node is severely affected by a shock. Voter models also can be extended so that a node, if selected, can not only adapt its state depending on the share of links to nodes of the other state, but also can adapt their links itself with other nodes [62, 57].

In the following chapter, we propose a data-driven adaptive extension to [31], inspired by the voter model as a bridge between the theoretical background from magnetism and the application in supply networks. The rule of this adaptation scheme will be much complex due to structure of the base model. Our take on the voter model will include a single variable status which is continuous, represented by the available amount of an item within a country. A shock is emitted by reducing the available amount of product of that node significantly or completely to zero. Every node that has either a trade or production link to the shocked node will be affected according to their individual trade and production function. In addition to that, if the reduction surpasses a relative loss threshold, the affected node will start to adjust weight and existence according to node specific rules. The network is extremely heterogeneous what also rubs off on to the adaptation rules. As we adapt the state and connections of multiple nodes at once, it will no longer be a single-flip, but multi-flip model. The intensity of how strongly the adaptation rules will be applied is determined by the node state. In summary, the adaptation possibilities will be local, node-specific, scaled by the severity of how harshly the node is affected by a shock and simultaneously applied to all affected entities. Due to the heterogeneity of the network and the intent to model the impact of shocks anywhere in the system systematically individually and as realistically as possible, we propose evolving from the rather simplistic toy model as the voter model to basing the system's adaptation empirically on in this case annual data of the global food production and trade network.

3 Model description

This chapter introduces the computational background of the proposed shock adaptation model for the food production and trade network. It serves as an extension to an existent model by Laber et al. [31] which enables modeling of shock propagation but with fixed trade and production strategies possible. The original model utilizes the FABIO data set [30], providing global multi-regional supply-use and input-output tables over 35 years. The dynamics of the system, from which the adaptation rules are derived, are based on the real-life trade and production adjustments of countries in response to actual events, combining directly observed changes and indirect correlations.

3.1 Data source

The FABIO database [30] spans 35 years, and for each of these years the parameters of the static model can be calculated as described in [31]. Our approach is based on comparing the parameters of two consecutive years. Consequently, we exclude any country that did not exist during the entire calibration period to avoid generating incorrect transition parameters due to non-existent data for some years. The data set starts in 1986, but we start our analysis in 1992 to take into account the significant geopolitical changes in 1991, in particular the dissolution of the Soviet Union and the emergence of 15 new states, including major agricultural players such as Russia and Ukraine.

The model parameters for the static model $\alpha^p_{a,i}$, $\beta^p_{a,i}$, $\nu^p_{a,i}$, T^i_{ab}, $\eta^{\text{exp}}_{a,i}$ and $\eta^{\text{prod}}_{a,i}$ and the initial vector ${x_0}^i_a$ as described in [31] are derived from the 2020 FABIO data, more specifically the supply, use and demand tables. Within the supply table, denoted $S_{(a,p),(b,i)}$, an entry describes the quantity of item i in area a supplied by process p in area b. In particular, $S_{(a,p),(b,i)} > 0$ only if $a = b$ for all $p \in \mathcal{P}$ and $i \in \mathcal{I}$, reflecting that areas supply only for their own needs. Moving on to the usage table, denoted as $U_{(a,i),(b,p)}$, each entry represents the amount of item i in area a used in process p in area b. Here, a and b can represent different areas. Finally, the demand table, labelled $Y_{(a,i),(b,k)}$, represents the quantity of item i in area a used for purpose k in area b. Purposes may include, but are not limited to, food, stocks, or additional processing not explicitly modelled. A full list of items, areas and processes included in the model can be found in the supplementary information (SI). The 2020 FABIO dataset comprises 192 countries (*areas*), denoted as $\mathcal{A}$, and a set of 123 agricultural products (*items*), denoted as $\mathcal{I}$, produced by 117 production processes (*processes*), denoted as $\mathcal{P}$. The exact derivation process is elaborated in [31]. The unique 2-tuple (a, i) of a country a and an item i is called a sector, resulting in a total of $23,616$ sectors.

To avoid unrealistic adjustments, we set a threshold of 10^{-3} for parameters denoting shares, which sometimes have extremely low values (e.g. 10^{-90} or lower). Parameters below this threshold are set to zero to ensure that the model creates new links rather than making disproportionate adjustments to negligible links.

3.2 Model without adaptation

We use a recent bipartite multilayer model of the propagation of food supply shocks [31] as our basic model. This model (Figure 3.1) quantifies the available amount of a product in a country, obtained through trade or production, through an iterative three-step process: production, trade and allocation. This process is repeated at each time step of the simulation. During production,

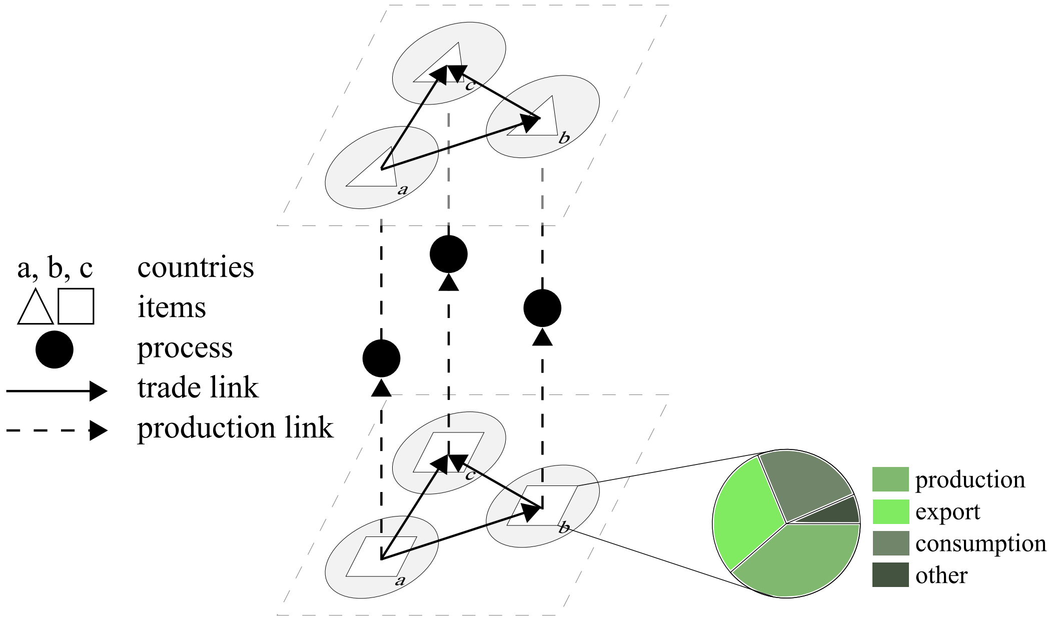

Figure 3.1: Schematic representation of the shock propagation model as a multilayer bipartite network of global food production and trade [31]. We show an example for three countries and two products. Each time step of the simulation goes through three iterative steps: trade, production and allocation. A layer represents a food product that can only be traded within the layer (trade links as solid arrows). Transitions between layers occur only through a production process (production process links as dashed lines). For each country-product combination, also called sector, fractions are individually allocated to different purposes (shown as a pie chart for an exemplary country-product combination). Note that each process may have several inputs and outputs, which are not explicitly shown here.

input products are transformed into output products through production processes; during trade, products are traded with other countries; and finally, during allocation, all products previously obtained through production or trade are allocated to different purposes for which they will be used in the next time step. The model allows the simulation of regional production shocks and observes direct and indirect losses in all (other) products and regions. The impact of shocks is measured by comparing the amount available in a shock scenario with the baseline case without shocks.

The output of a sector (a, i), referring to an item i in an area a, is quantified by summing the outputs of each production process p that produces the item. $\alpha^p_{a,i}$ represents the output rate of processes p to sector (a, i) that require inputs according to the model, while $\beta^p_{a,i}$ covers processes that can produce without food inputs. Either $\alpha^p_{a,i}$ or $\beta^p_{a,i}$ can be greater than zero for any combination of a,i and p, but not both. Processes with $\beta^p_{a,i} > 0$ typically refer to the harvesting of primary agricultural products where seed is not recorded as an input. The input share for process p of the share allocated to production of sector (a, j) $p^j_a(t-1)$ is denoted by $\nu^p_{a,j}$, resulting in output $o^i_a(t)$:

$$o^i_a(t) = \sum_{p\in\mathcal{P}} (\alpha^p_{a,i} \sum_{j\in\mathcal{I}} (\nu^p_{a,j} p^j_a(t-1)) + \beta^p_{a,i}) \quad . \tag{3.1}$$

The amount obtained from trade $h^i_a(t)$ is calculated by summing the imports from trading partners from which item i is imported. T^i_{ab} indicates the shares of the for-trade reserved volumes $e^i_b(t-1)$

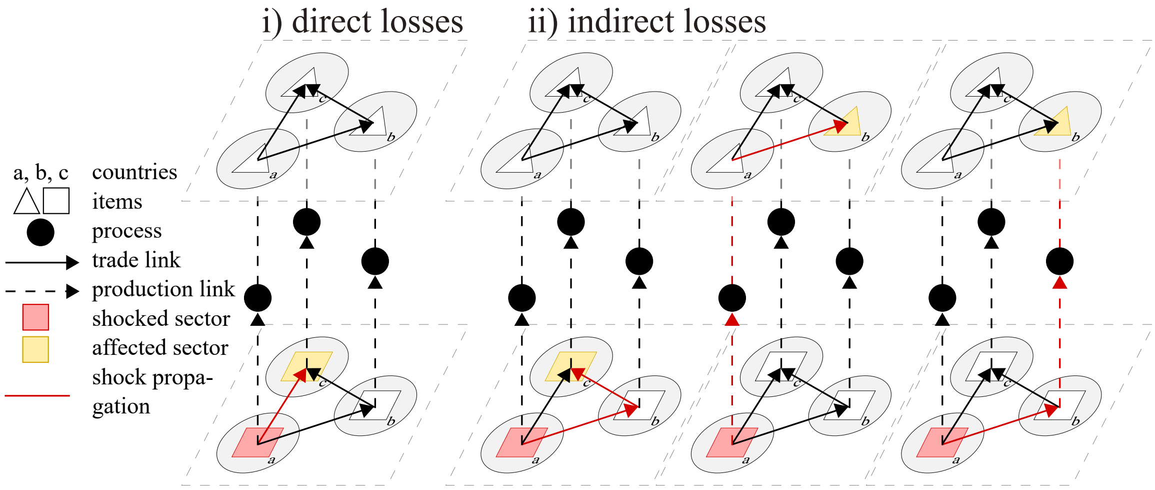

Figure 3.2: Shock propagation through the model [31] allows for four types of shock transmission (i). Direct losses at $t = 1$ occur immediately after the shock to production at $t = 0$, which can only affect direct trading partners (ii). These direct effects can propagate within a layer of the trade network and lead to indirect trade losses in third countries (first figure). Other items may also suffer losses, either because production in the shocked area and hence trade in the secondary item is affected (second figure), or because production in the receiving areas is affected (third figure).

of exporting sector (b, i) that are to be received by country a:

$$h_a^i(t) = \sum_{b \in \mathcal{A}} T_{ab}^i e_b^i(t-1) \quad . \tag{3.2}$$

At the end of a time step t, sector (a, i) has a total amount $x_a^i(t)$ available:

$$x_a^i(t) = o_a^i(t) + h_a^i(t) \quad . \tag{3.3}$$

$p_a^i(t)$ and $e_a^i(t)$ are the shares of $x_a^i(t)$ allocated to production and exports respectively, according to the individual shares η of each sector:

$$p_a^i(t) = \eta_{a,i}^{\text{prod}} \cdot x_a^i(t) \quad , \tag{3.4}$$

$$e_a^i(t) = \eta_{a,i}^{\text{exp}} \cdot x_a^i(t) \quad . \tag{3.5}$$

A shock to the system is induced by artificially destroying a fraction ϕ or all ($\phi = 100\%$) of the output of item i in area a at time step t, starting at $t = 0$ until the end of the simulation $t = \tau$:

$$o_a^i(t) = (1 - \phi) \cdot o_a^i(t) \quad \forall t \in \{0, ..., \tau\} \quad . \tag{3.6}$$

The shock propagates through the production and trade network. The model captures not only direct losses due to first-order trade relationships of the shocked area and its direct customers, but also quantifies indirect losses resulting from higher-order trade relationships (Figure 3.2). It also covers the indirect effects on secondary items that use the initially shocked item upstream in their production. The loss $L_{a \to b}^{i \to j}(t)$ of a sector (b, j) due to a shock to sector (a, i) at time t is assessed as an absolute per capita loss relative to the baseline, which is a scenario $\underline{x}$ of the simulation in which no shock was issued:

$$L_{a\to b}^{i\to j}(t) = \frac{\underline{x}_b^j(t) - x_{a\to b}^{i\to j}(t)}{z_b} \quad . \tag{3.7}$$

$x_{a\to b}^{i\to j}(t)$ is the amount available in sector (b, j) after a shock to sector (a, i), while $\underline{x}_b^j(t)$ is the availability in sector (b, j) in the unshocked scenario. z_b is the population of recipient country b in the year 2020 as reported by [63]. We will usually use $L_{a\to b}^{i\to j} = L_{a\to b}^{i\to j}(\tau)$ where $\tau = 10$ is the length of a simulation run and $L_{a\to b}^{i\to j}$ is the final absolute loss per capita, which serves as an indicator of the severity of a shock.

3.3 Extending the dynamical model with adaptation rules

As the parameters used by the static model are fixed, countries cannot respond to major shocks in their upstream supply chain. Even major disruptions that cause high direct losses, which may lead to further losses in secondary products, are not met with adapted production, trade or allocation strategies that could potentially mitigate or even eliminate the initial losses, or at least prevent additional indirect losses. The static approach does not fully capture the dynamics of shock propagation in the food production and trade network. In reality, the network is not static, and especially in times of distress, affected entities tend to seek alternative strategies to improve their situation [38, 32, 26, 39, 29], as in the case of COVID-19, where food supply chains held up remarkably well[64]. As the static model is based on three steps that each country performs within each time step, affected countries can adjust these three steps accordingly. We explore this in more detail by looking at the potential adaptations of Bangladesh after a shock to Indian rice production (Figure 3.3). Some possible solutions for how Bangladesh could mitigate its losses include

- Increase the volume of imports by strengthening existing or establishing new trade relationships in the vulnerable product: In this example, Bangladesh could seek to import more from another major rice exporter such as Thailand (Figure 3.3 a I).
- Adjust the allocation of production inputs, for example by directing more of the vulnerable product to its own production as seed or regular inputs (i.e. grain as input for livestock versus grain as input for more grain production, Figure 3.3 a II i), or by increasing the absolute rate of production in the case of inefficiencies (Figure 3.3 a II ii).
- Shifting allocation from trade to domestic uses such as production or consumption: In particular, exporting a significant proportion of the affected good may exacerbate the shortage (Figure 3.3 a III).
- Increased imports of suitable substitutes: Bangladesh may not be able to mitigate rice losses, but it could try to import substitutes, e.g. other cereals such as maize, which can be used for the same or similar purposes and production processes, and thus at least mitigate losses on affected common secondary products, such as live animals in this case (Figure 3.3 b).

Typically, a country does not pursue the most effective supply strategy when improving resilience, as efficiency and resilience in supply chains prove to be contradictory [64]. When a major global supplier experiences a shock, a significant proportion of a product is typically removed from the system, and since the system is closed, no new resources can be added to fully compensate for the losses. In the following sections, we provide a data-driven extension to the static model that allows countries to adapt to their situation and compensate for their losses in a way that replicates real-world behaviour.

3.3.1 Growth adjustment

As the focus is on the adaptive behaviour of countries by changing their trade and production strategy, the parameters obtained from the FABIO data [30] are adjusted for the effects of economic

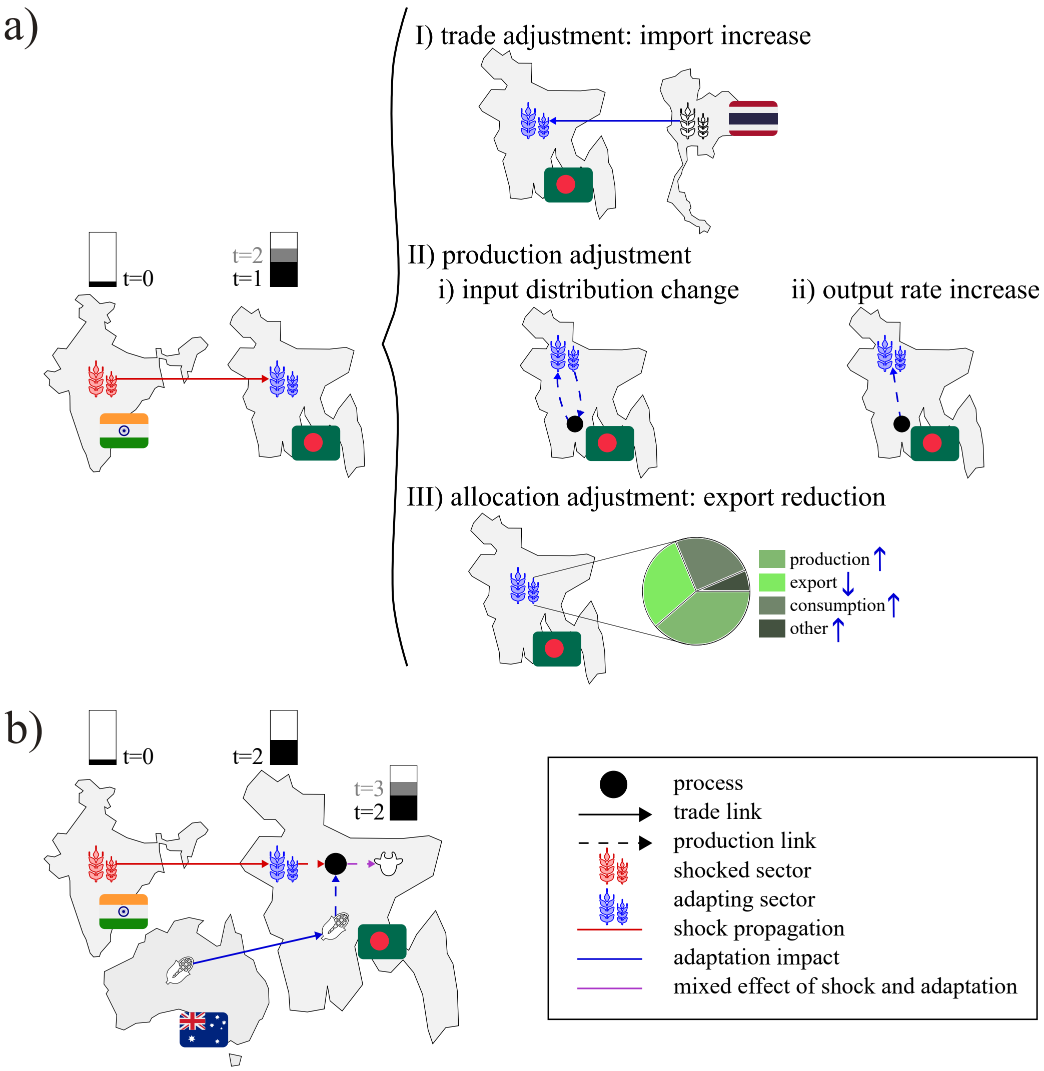

Figure 3.3: Schematic illustration of adaptation strategies with (a) direct adaptations and (b) indirect adaptations allowing product substitution strategies. In panel (a), an initial shock to the availability of rice in India is shown in red and by a bar that reaches zero, indicating a complete loss of availability. The shock propagates through trade and production linkages. For example, if Bangladesh experiences a substantial reduction in rice availability (blue), as indicated by the lower level of the bar at $t = 1$, this triggers the adjustment mechanism to mitigate the losses from $t = 2$ onwards. Possible beneficial adjustments include: (I) changing trade links to import the missing product from alternative sources such as Thailand, (II) adjusting production links to (i) allocate more of the product to self-replicating processes or (ii) increase production of the missing item from other processes, and (III) changing the allocation scheme to reduce exports and increase production or consumption. In panel (b), if Bangladesh also continues to experience reduced availability of rice at $t = 2$, it has the additional option of importing substitute products, here maize, that can be used in similar production processes from a trading partner, here Australia, thereby mitigating the impact on secondary products, such as live animals, which can be fed either rice or maize, from $t = 3$ onwards. Credits: flags: SVG Repo under MIT licence; country shapes and food icons: SVG Repo under no licence

growth. Since the parameters $\nu^p_{a,i}$, T^i_{ab}, $\eta^{\text{exp}}_{a,i}$ and $\eta^{\text{prod}}_{a,i}$ denote shares and cannot lead to volume increases that would indicate economic growth, they do not need to be adjusted. $\alpha^p_{a,i}$ and $\beta^p_{a,i}$, the output rates of production processes with or without quantifiable inputs, are expressed in absolute terms and can therefore reflect economic growth. To eliminate this effect, we ensure that the output volume of a process p is constant across all its production sectors (a,i). The parameters $\alpha^p_{a,i}$ and $\beta^p_{a,i}$ calculated for the base year 1992 are used as a reference. We calculate the normalised version $\alpha^p_{a,i,\text{norm}}(T)$ and $\beta^p_{a,i,\text{norm}}(T)$ from the unnormalized original parameters $\alpha^p_{a,i,\text{unnorm}}(T)$ and $\beta^p_{a,i,\text{unnorm}}(T)$ for each year T:

$$\alpha^p_{a,i,\text{norm}}(T) = \alpha^p_{a,i,\text{unnorm}}(T) \cdot \frac{\sum\limits_{i\in\mathcal{I}} \alpha^p_{a,i,\text{unnorm}}(1992)}{\sum\limits_{i\in\mathcal{I}} \alpha^p_{a,i,\text{unnorm}}(T)} \quad , \tag{3.8}$$

$$\beta^p_{a,i,\text{norm}}(T) = \beta^p_{a,i,\text{unnorm}}(T) \cdot \frac{\sum\limits_{i\in\mathcal{I}} \beta^p_{a,i,\text{unnorm}}(1992)}{\sum\limits_{i\in\mathcal{I}} \beta^p_{a,i,\text{unnorm}}(T)} \quad . \tag{3.9}$$

In short, from now on we will use $\alpha^p_{a,i}(T) = \alpha^p_{a,i,\text{norm}}(T)$ and $\beta^p_{a,i}(T) = \beta^p_{a,i,\text{norm}}(T)$.

The initial vector $x_0{}^i_a$ is also rescaled by the total amount of globally available items in 1992, as the absolute amount available may also reflect economic growth. The rescaled initial vector $x_0{}^i_{a,\text{norm}}(T)$ is calculated from the original initial vector $x_0{}^i_{a,\text{unnorm}}(T)$ for each year T in the calibration, holding the total amount of available products across all sectors constant:

$$x_0{}^i_{a,\text{norm}}(T) = x_0{}^i_{a,\text{unnorm}}(T) \cdot \frac{\sum\limits_{(a,i)\in\mathcal{A}\times\mathcal{I}} x_0{}^i_{a,\text{unnorm}}(1992)}{\sum\limits_{(a,i)\in\mathcal{A}\times\mathcal{I}} x_0{}^i_{a,\text{unnorm}}(T)} \quad . \tag{3.10}$$

For brevity, we set $x_T{}^i_a = x_0{}^i_{a,\text{norm}}(T)$.

3.3.2 Event definition

Sectors that have historically lost a significant amount of available quantity from one year to another are identified as follows. Where (a_E, i_E) is the event sector, T_E is the time of an event and l_E is the relative loss of available quantity of the sector at $T = T_E$. To be classified as an event, the 4-tuple (a_E,i_E,T_E,l_E) must satisfy three criteria:

- substantial relative loss of available amount $\Delta^{a_E,i_E,T_E}_{rel}$ exceeding the threshold limit Δ_{rel}:

$$\Delta^{a_E,i_E,T_E}_{\text{rel}} = \left| \frac{x_{T_E}{}^{i_E}_{a_E} - x_{(T_E-1)}{}^{i_E}_{a_E}}{x_{(T_E-1)}{}^{i_E}_{a_E}} \right| > \Delta_{\text{rel}} \tag{3.11}$$

  with $\Delta^{a_E,i_E,T_E}_{\text{rel}} = l_E$.

- substantial absolute loss of available amount $\Delta^{a_E,i_E,T_E}_{\text{abs}}$ exceeding the threshold limit Δ_{abs}:

$$\Delta^{a_E,i_E,T_E}_{\text{abs}} = \left| x_{T_E}{}^{i_E}_{a_E} - x_{(T_E-1)}{}^{i_E}_{a_E} \right| > \Delta_{\text{abs}} \quad . \tag{3.12}$$

- Stable conditions before and after the event. To quantify stability, the coefficient of variation (CV) is used and must fall below the threshold Δ_{dev}:

$$CV = \frac{\sigma}{\mu} < \Delta_{\mathrm{dev}} \tag{3.13}$$

$$\text{with} \quad \mu = \langle x_{T}{}^{i_E}_{a_E} \rangle_T \quad \text{and} \quad \sigma = \sqrt{\langle (x_{T}{}^{i_E}_{a_E})^2 \rangle_T - \mu^2} \quad . \tag{3.14}$$

  If the CV for either $T < T_E$ or $T > T_E$ exceeds the threshold Δ_{dev}, then the event (a_E, i_E, T_E, l_E) is not considered relevant. To apply this criterion sensibly, potential events with $T_E < 1997$ or $T_E > 2015$ will not be considered, as there will be too few years before or after the event to quantify stability. We need at least 5 years to evaluate this criterion. Furthermore, because of this aspect, each starting entry time series can only contain one potential event, otherwise the rest of the time series couldn't be stable.

The resulting subset of relevant events can now be used to determine adaptation strategies as parameter changes related to the event sector at the time of the event.

3.3.3 Calibration of adaptation rules

Changes in each of the model parameters $\alpha^p_{a,i}$, $\beta^p_{a,i}$, $\nu^p_{a,i}$, T^i_{ab}, $\eta^{\mathrm{exp}}_{a,i}$ and $\eta^{\mathrm{prod}}_{a,i}$ after a relevant event identified in 3.3.2 are observed to derive general adjustment rules. The framework of possible post-event adjustments for an example parameter entry v describes the change with a weight adjustment component w and a rewiring component r. In the following, l_E represents the loss of an example event E. We have:

$$v(T_E + 1) = l_E \cdot w \cdot v(T_E) + l_E \cdot r \quad . \tag{3.15}$$

The weight adjustment and the rewiring component can be calculated as follows, since l_E and the variable v are known before and after the event:

$$w = \begin{cases} \frac{1}{l_E} \frac{v(T_E+1)}{v(T_E)}, & \text{if } v(T_E) > 0 \\ 0, & \text{if } v(T_E) = 0 \end{cases} \quad , \tag{3.16}$$

$$r = \begin{cases} 0, & \text{if } v(T_E) > 0 \\ \frac{1}{l_E} v(T_E), & \text{if } v(T_E + 1) = 0 \end{cases} \quad . \tag{3.17}$$

For an event (a_E, i_E, T_E, l_E), the observed changes in an entry of the production output rate α related to that event result in the following adjustment components:

$$w_{\alpha^p_{a_E,i_E}} = \begin{cases} \frac{1}{l_E} \frac{\alpha^p_{a_E,i_E}(T_E+1)}{\alpha^p_{a_E,i_E}(T_E)}, & \text{if } \alpha^p_{a_E,i_E}(T_E) > 0 \\ 0, & \text{if } \alpha^p_{a_E,i_E}(T_E) = 0 \end{cases} \quad , \tag{3.18}$$

$$r_{\alpha^p_{a_E,i_E}} = \begin{cases} 0, & \text{if } \alpha^p_{a_E,i_E}(T_E) > 0 \\ \frac{1}{l_E} \alpha^p_{a_E,i_E}(T_E), & \text{if } \alpha^p_{a_E,i_E}(T_E + 1) = 0 \end{cases} \quad . \tag{3.19}$$

For each individual combination of event sector (a_e, i_e), a specific weight adjustment $m_{\alpha^p_{a_E,i_E}}$ and a rewiring adjustment $r_{\alpha^p_{a_E,i_E}}$ can be determined. For increased robustness and coverage, adaptation rules for collections of events are inferred by averaging over all countries a_E for which a substantial event has been observed for item i_E:

$$W_{\alpha^{\ p}_{i_E}} = \langle w_{\alpha^{\ p}_{a_E,i_E}} \rangle_{a_E} \qquad \Rightarrow \quad W_{\alpha^{\ p}_{i_E}} = W\alpha^{p}_{a,i_E} \qquad \forall a \in \mathcal{A} \quad , \tag{3.20}$$

$$R_{\alpha^{\ p}_{i_E}} = \langle r_{\alpha^{\ p}_{a_E,i_E}} \rangle_{a_E} \qquad \Rightarrow \quad R_{\alpha^{\ p}_{i_E}} = R_{\alpha^{\ p}_{a,i_E}} \qquad \forall a \in \mathcal{A} \quad . \tag{3.21}$$

For β and ν, the weight adjustment and the rewiring transformation matrix can be derived in the same way. The allocation parameters are also derived in a similar way, as the values are aggregated to obtain a full vector, assuming similar item adjustment behaviour across countries. The trade parameter, on the other hand, describes country-country relationships, not item-process relationships, and therefore averaging across event countries eliminates relevant information. When completing the transformation parameter for the trade parameter in the direction of imports, the aggregation over all items is carried out by averaging over all items i_E for which a substantial event was observed in area a_E:

$$W_{T_{a_E b}} = \langle w_{T^{\ i_E}_{a_E b}} \rangle_{i_E} \qquad \Rightarrow \quad W_{T_{a_E b}} = W_{T^{\ i}_{a_E b}} \qquad \forall i \in \mathcal{I} \quad , \tag{3.22}$$

$$R_{T_{a_E b}} = \langle r_{T^{\ i_E}_{a_E b}} \rangle_{i_E} \qquad \Rightarrow \quad R_{T_{a_E b}} = R_{T^{\ i}_{a_E b}} \qquad \forall i \in \mathcal{I} \quad . \tag{3.23}$$

The export direction is derived in a similar way, but instead of changes from $T_{a_E b}(T_E)$ to $T_{a_E b}(T_E + 1)$, we observe changes from $T_{b a_E}(T_E)$ to $T_{b a_E}(T_E + 1)$ when evaluating the impact of event (a_E,i_E,T_E,l_E).

3.3.4 Implementation of adaptation rules

In the simulation, the adaptation of a parameter entry v_{orig}, which contains $\alpha^p_{a,i}$, $\beta^p_{a,i}$, $\nu^p_{a,i}$, T^i_{ab}, $\eta^{\text{exp}}_{a,i}$ and $\eta^{\text{prod}}_{a,i}$, calculated on the basis of the data for 2020, the latest available year, by means of a weight adjustment w and a rewiring r after its associated sector (a_S, i_s) has experienced a relative loss l_S at $t = 1$, one time step after the initialisation of the shock, the simulation is applied as follows and results in v_{adap}:

$$v_{\text{adap}} = l_S \cdot w \cdot v_{\text{orig}} + l_S \cdot r \quad . \tag{3.24}$$

Using the example of the production output parameter α again, and applying the adaptations derived in (3.18) to (3.21), the resulting parameter is:

$$\alpha^p_{a_S,i_S,\text{adap}} = l_S \cdot W_{\alpha^{\ p}_{a_S,i_S}} \cdot \alpha^p_{a_S,i_S,\text{orig}} + l_S \cdot R_{\alpha^{\ p}_{a_S,i_S}} \quad . \tag{3.25}$$

l_S, the relative loss in available amount, must exceed the same limit Δ_{rel} as the events defined in (3.11). The absolute loss in available amount must also exceed the absolute event definition limit Δ_{abs} as in (3.12). All nodes that satisfy these two criteria, denoted by 3-tuples (a_S,i_S,l_S), adjust their associated parameters at $t = 1$. The parameters remain in the adapted state for the rest of the simulation, allowing the system to reach a stable state after a few time steps.

The adjustment rules fulfil a number of constraints. Entries in the trade matrix that would transform an item i into an item j when exported from country a to country b are always kept at 0, as are entries in the output matrix that would denote an output item i from a process p in country a to another country b.

The sum over all exports of an item originating in a country must equal one, so the rows in $T^i_{ab,\text{adap}}$ are rescaled so that the ratio between the amounts received by different importers b and the total amount exported by exporter a remains constant:

$$T^i_{ab,\mathrm{adap,norm}} = \frac{T^i_{ab,\mathrm{adap}}}{\sum\limits_{(b,i)\in(\mathcal{A}\times\mathcal{I})} T^i_{ab,\mathrm{adap}}} \quad . \tag{3.26}$$

The production input parameter ν must satisfy a similar constraint, ensuring that no more than 100% of an available product allocated for production is spent on production processes:

$$\nu^p_{a,i,\mathrm{adap,norm}} = \frac{\nu^p_{a,i,\mathrm{adap}}}{\sum\limits_{(a,p)\in(\mathcal{A}\times\mathcal{P})} \nu^p_{a,i,\mathrm{adap}}} \quad . \tag{3.27}$$

The shares that allocate the available amounts to different purposes cannot accumulate above or below one, so the shares associated with each purpose k are scaled accordingly:

$$\eta^k_{a,i,\mathrm{adap,norm}} = \frac{\eta^k_{a,i,\mathrm{adap}}}{\sum\limits_{k} \eta^k_{a,i,\mathrm{adap}}} \quad . \tag{3.28}$$

The total output rate of a production process p in country a for all its products i is held constant at its original level:

$$\alpha^p_{a,i,\mathrm{adap,norm}} = \alpha^p_{a,i,\mathrm{adap}} \frac{\sum\limits_{(a,p)\in(\mathcal{A}\times\mathcal{P})} \alpha^p_{a,i,\mathrm{orig}}}{\sum\limits_{(a,p)\in(\mathcal{A}\times\mathcal{P})} \alpha^p_{a,i,\mathrm{adap}}} \quad , \tag{3.29}$$

$$\beta^p_{a,i,\mathrm{adap,norm}} = \beta^p_{a,i,\mathrm{adap}} \frac{\sum\limits_{(a,p)\in(\mathcal{A}\times\mathcal{P})} \beta^p_{a,i,\mathrm{orig}}}{\sum\limits_{(a,p)\in(\mathcal{A}\times\mathcal{P})} \beta^p_{a,i,\mathrm{adap}}} \quad . \tag{3.30}$$

3.3.5 Item substitutability

Product substitutability is inferred from correlations between local losses in one product and import surges in another similar product. Products are considered similar, and therefore potential substitutes, if they belong to the same commodity group. Given the set of relevant events (a_E,i_E,T_E,l_E) derived in 3.3.2, we first define a general trade import index $I^j_{a_E}$ for each item j similar to event item i_E in event country a_E by summing over all relevant import indices. To be included in the sum, the sector (a_E, i_E) must be a significant importer from (b, i_E) in question, receiving at least 0.1 % of the sector's exports:

$$I^j_{a_E}(T_E) = \sum_b T^j_{a_E b}(T_E) \quad . \tag{3.31}$$

We derive the mean relative change in this trade-import index with respect to j by averaging over all events affecting sectors of item i_E, giving the substitutability index $s_{i_E j}$ as

$$s_{i_E j} = \left\langle \frac{I^j_{a_E}(T_E+1) - I^j_{a_E}(T_E)}{I^j_{a_E}(T_E)} \right\rangle_{a_E, j\neq i_E} \quad . \tag{3.32}$$

The substitution rule is only considered in the model if the following null hypothesis H^A_0 is rejected,

$$H^A_0: \quad s_{i_E j} \leq 0 \quad . \tag{3.33}$$

In addition, a permutation test ensures the consistency of the results by randomly permuting over the distribution of event item-area combinations and correcting the resulting p-values using the Benjamini-Hochberg correction method [65] to mitigate errors associated with multiple testing. The second null hypothesis H_0^B tests whether the mean of the permutations of $s_{i_E j}$ is less than 0,

$$H_0^B : \quad \langle s_{i_E j} \rangle_{\mathrm{perm}} \leq 0 \quad . \tag{3.34}$$

For both null hypotheses, the significance level is set at $p < 0.05$. Since we are deriving an item $\times$ item size substitutability matrix s, to apply it to the trade parameter we inflate the size by applying the substitution scheme to each country a, resulting in the full substitutability index matrix S:

$$s_{i_E j} = S^a_{i_E j} \quad \forall a \in \mathcal{A} \quad . \tag{3.35}$$

The substitutability index adjustment is applied when a sector has lost a significant proportion and quantity of its available goods and has not been able to recover through the adjustment applied at $t = 1$. The substitutability indices are applied at $t = 2$ in addition to the first round of adjustments. They are applied according to the same criteria as in 3.3.4, which are derived from (3.11) and (3.12), to all entries that define the import parameters to the affected sector (a_S, i_S) for which j could serve as a substitute:

$$T^j_{a_S b,\mathrm{adap}} = (1 + S^a_{i_S j}) \cdot T^j_{a_S b,\mathrm{orig}} \quad . \tag{3.36}$$

$T^j_{a_S b,\mathrm{orig}}$ represents the current iteration of the trade matrix as the result $T^j_{a_S b,\mathrm{adap,norm}}$ obtained after (3.26) in the previous time step. This method only adapts existing trade relations. This preserves the item-blocked structure of the trade matrix. However, (3.26) must be reapplied to the result of (3.36) to ensure that there are no forbidden gains or losses of goods within the trade.

4 Results

With the model covering 123 products in 192 countries, a total of 23616 possible shock scenarios could theoretically be observed. However, given that not every country produces and exports every single product, a shock to certain combinations would have no or very little effect. Taking this into account, we are left with 5450 in possible shock scenarios. Of these, only 2558 worth of combinations belong to the 'primary crops' product group. Shortages in this category affect not only the availability of the shocked product itself, but also secondary products derived from production processes that initially require primary products as inputs. In this chapter, after discussing the results from the event definition and time stability of the derived microscopic adjustment rules and highlighting the most relevant ones, we will further examine an exogenous shock to rice production in India and wheat production in Ukraine and its macroscopic effects. In addition, we will examine the superposition of these two large shocks. Both shocks are among the potentially most impactful and are inspired by current events of the last two years.

4.1 Food Availability Shocks in the Real World

To derive meaningful and stable adjustment rules, we base them on events that have had a significant impact on food availability in a given region. Let ${x_T}_a^i$ denote the quantity available within sector (a, i) in year T. For an event to qualify, it must simultaneously meet three criteria, as described in section 3.3.2.

A hyperparameter search combined with a train/test split of the data was performed to identify the set of thresholds that would result in a robust set of adjustment rules, while balancing the number of sectors for which rules could be identified. We found that $\Delta_{\text{rel}} = 0.26$, $\Delta_{\text{abs}} = 1000$ tonnes and $\Delta_{\text{dev}} = 0.32$ is the optimal setting to cover almost the entire network with reasonably stable adjustment rules. If the adjustment rules prove to be stable over time, it is reasonable to assume that they can also be used to estimate future compensation. To test their stability over time, the years for which the data set is available are divided into two parts. The first part is from 1992 to 2006 and the second part from 2006 to 2020. The derivation of the adjustment rules, including 3.3.2 and 3.3.3, is performed for the event years at the beginning and end of each section, which are reduced from five to three years. This adjustment ensures that each section has eight years instead of four as potential event times for comparison. The resulting correlation coefficients between the two resulting transformation matrices for each parameter (both multiplier and rewiring adjustment) are calculated for different sets of event definition limits and then compared to obtain the optimal limit. The final event limits should also take into account that there are enough relevant events within the limits to cover all 192 countries and 123 products included in the model, while ensuring that the computational time remains reasonable.

To find the optimal limit, we first analyse the general trends when varying the limits for the three event criteria. Keeping the absolute limit as low as possible results in the highest number of events and also shows the steepest decline in events. We choose 1000 tonnes as the absolute limit because it is rather low compared to the largest observed amounts available in the model, which can reach up to 1.5×10^{10} tonnes, but it will exclude some minor fluctuations that account for only a few tonnes. The distributions for the relative and deviation limits show the steepest decreases and increases around 0.26 and 0.32 respectively. For these bounds, the number of events is also sufficiently high over the whole and the two separate periods of observation. Keeping one of the bounds

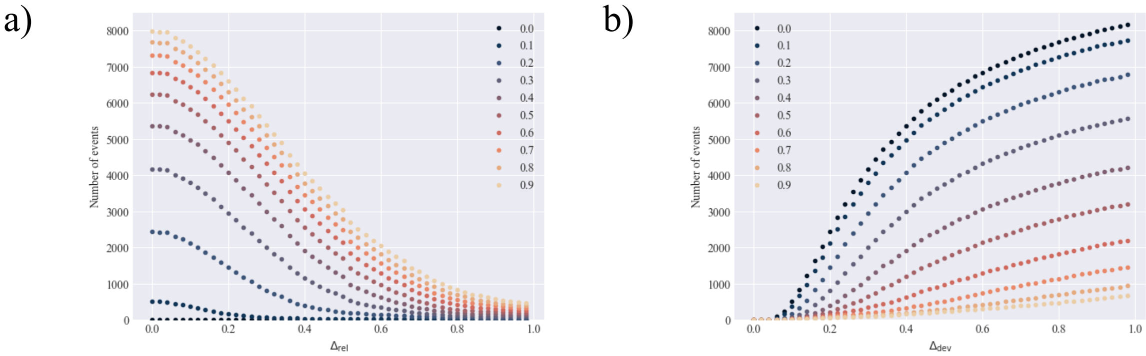

Figure 4.1: Number of events for different sets of relative drop and deviation limits (a). The relative limit is varied from 0 to 1 for different levels of allowed deviation from 0.0 to 0.9 (b). The deviation limit is varied from 0 to 1 for different levels of the relative drop limit from 0.0 to 0.9. In general, the lower the relative drop limit and the higher the allowed deviation limit, the more relevant events can be observed. There is no clear transition point where the shape of the distribution changes, but the average steepest decline is observed for a relative drop limit of 0.26 and the average steepest rise is observed for an allowed deviation limit of 0.32.

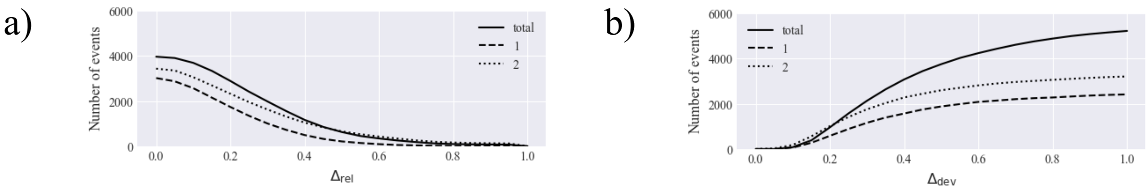

Figure 4.2: Number of events within different time frames for different sets of relative drop and deviation limits: On the left, the allowable deviation limit is set to 0.32 and the relative limit is varied from 0 to 1. On the left, the relative drop limit is set to 0.26 and the deviation limit is varied from 0 to 1. Both distributions show that the combination of a deviation limit of 0.32 and a relative limit of 0.26 provides a high enough number of events for the total and both parts of the split period with counts well above 1000.

in question fixed, while varying the other from 0.1 to 0.7, the fitting matrices for each parameter are calculated for both parts of the separated time period. For each pair of identical bounds and parameters, the Matthews correlation [66], a measure of binary association, is determined. This type of correlation measure does not take into account the size of an entry in the transition matrix; rather, it assesses whether an entry exists by measuring the correlation of whether a rule itself is present in both, neither, or only one section. The matrices derived by the method introduced in 3.3.3 show a high to very high correlation for every kind of combination of boundary definitions. Only the substitutability index 3.3.5 is not highly correlated over the whole range of boundaries and only reaches moderate correlation for relative drop boundaries below 0.3 and allowed deviation boundaries above 0.3, corresponding to our initially chosen values of $\Delta_{\mathrm{rel}} = 0.26$ and $\Delta_{\mathrm{dev}} = 0.32$.

We obtain more than $2,300$ relevant events from $23,616$ time series, covering 120 of the 123 food items and 177 of the 192 countries. We find that most of the adjustment parameters have a high Matthew correlation coefficient M between their values in the training and test data, ranging from 0.5 to 0.9, with item substitutability being the only exception, showing moderate correlation values for both relative bounds and deviation bounds, ranging from 0.2 to 0.4.

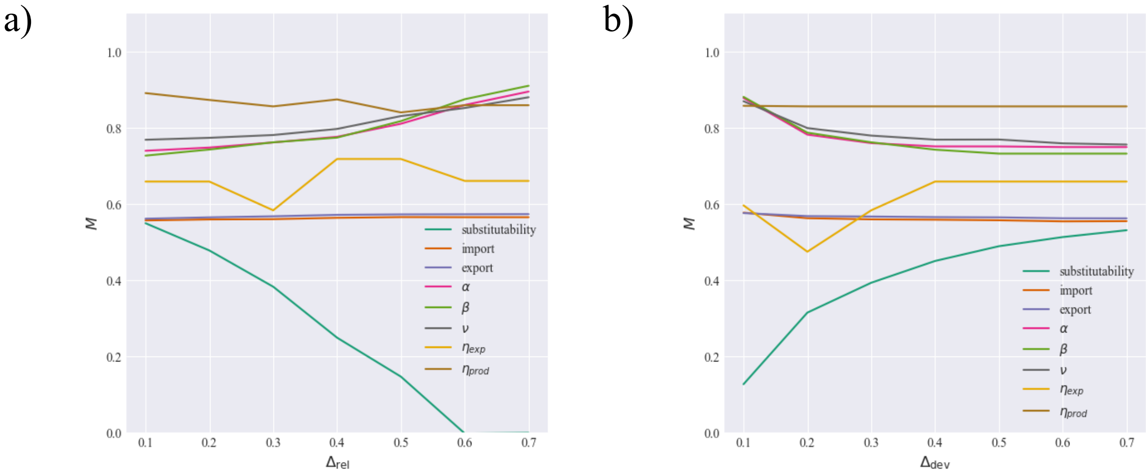

Figure 4.3: Matthews correlation of the adaptation matrices of both time sections for varying (a) relative limit and (b) deviation limit. The substitution index (3.3.5) is the least correlated adaptation parameter across both bounds. For varying the relative limit (while keeping $\Delta_{\text{dev}} = 0.32$), the Matthews correlation for the substitution index falls below 0.4, which we consider to be the threshold for moderate correlation, between 0.2 and 0.3, while all other adaptation matrices show strong to very strong correlation throughout. For varying deviation (keeping $\Delta_{\text{rel}} = 0.26$), the substitution index again shows the weakest correlation, exceeding 0.4 around 0.3. The other adaptation matrices again show moderate to high correlations throughout.

4.2 Overview of most relevant adaptation rules

We can derive the same number of adaptation matrices as the parameter matrices used by the static model. However, similar to the original parameter matrices, these adaptation matrices will not have an entry for every combination of domain, item and process, as not every combination has a valid adaptation rule. Table 4.1 provides an overview of the number of entries that could potentially adapt an original entry in a parameter matrix in the event of a shock, if the related unit experiences a significant loss. For the multiplication adjustment, relevant adjustments are indicated by entries not equal to 1, while for the rewiring adjustment, relevant adjustments are indicated by entries not equal to 0. The trade parameter adjustments, both in the import and export direction, have the highest number of possible adjustment rules, with relevant entries in their multiplier adjustment matrices exceeding 2.5 million, which significantly exceeds the number of possible adjustments for production parameters. In the model, every country is allowed to trade with every other country. On the other hand, production parameters are highly restricted. Only certain products can be used as inputs in certain production processes. For example, only the product `Pigs` and not other animals such as `Poultry`, `Sheep` or `Rabbits and hares` can be used as inputs in the process `Slaughtering pigs`. Similarly, the output side of processes tends to be even more restricted. For example, the process `Beverage production, fermented` can use all kinds of fruits and grains as inputs, but can only supply the product `Beverage production, fermented`. The allocation vectors η^{prod} and η^{exp} are only 23616×1 in size, unlike the other parameters, which are 23616×23616 matrices for trade and 23616×22656 for production. Due to their much smaller size, their adaptation matrices can only represent a much smaller number of possible changes.

Table 4.1: Number of rules for each adaptation method. For each parameter, except η_{exp}, the number of possible multiplication adaptations is at least one order of magnitude greater than the number of rewiring adaptations. We observe the largest number of possible applicable rules for both directions of trade parameters.

Variable	**Number of multipliers**	**Number of rewirers**
T (import)	2.786.934	803.190
T (export)	2.914.484	876.744
α	22.080	2.304
β	21.120	384
ν	169.728	29.568
η^{exp}	21.696	10.368
η^{prod}	14.208	2.496

Table 4.2: Overview of effective adjustment rules. We show the top 10 most impactful import trade weight adjustment multipliers. W_{Tab} is the multiplier for the existing trade relationship from country a to country b if any product in country a experiences a significant shortage, according to the estimated impact ι_{ab}.

Import country	**Export country**	$\boldsymbol{W_{Tab}}$	**Estimated impact $\boldsymbol{\iota_{ab}}$ in $\mathbf{10^6}$ tons**
Netherlands	Germany	3.69	8.05
Syrian Arab Republic	Turkey	13.31	5.46
Guatemala	El Salvador	8.63	3.96
China, mainland	United States of America	9.18	3.46
Romania	Hungary	7.34	3.45
Germany	Netherlands	2.29	1.99
Germany	Denmark	4.47	1.83
Afghanistan	Pakistan	1.77	1.53
China, mainland	Thailand	5.14	1.52
China, mainland	Brazil	1.45	1.25

We consider two classes of adaptation rules, multiplying (changing the weight of network links) or rewiring (creating new links). Comparing the number of rules discovered, multiplication is much more common than rewiring (Table 4.1), although each of the matrix pairs is based on the same set of parameter matrices and could therefore in principle have the same number of adaptation rules. Existing trade agreements, knowledge on topics such as regulatory environment and business practices and political and diplomatic ties make strengthening existing partnerships less time consuming and costly and therefore more favorable. New trade partnerships usually require significant initial investments e.g. to build transportation capacities and quality controls. Hence, there are far more opportunities for weight adjustments of existing trade relations than to create new ones which we focus on below.

4.2.1 Most important trade adaptations

Since the trade adjustment matrix is first derived at the country level as the average behaviour over all products, the trade adjustment rules for each product are the same from country to country. Figure 4.4 shows the trade adjustment multiplier matrix at the country level. The highest observed multiplier is 487 for imports from Oman to Somalia. As the original trade matrices on which the adjustment rules are based contain values up to several negative powers of ten, the application of such a high multiplier may not directly lead to extremely high import levels. In addition, the trade matrix is renormalized after the adjustment according to the equation (3.26), so that the sum of all export shares of a country-product combination always equals 1. If a country originally received a share of another country's exports as imports, and this share is not multiplied by an adjustment parameter of 0, then it will eventually retain some import shares after adjustment, even if other countries scale the import share by extremely large amounts. However, these cases are rather rare; the mean for increasing multipliers is only 3.2 and the mean for decreasing multipliers is around 0.48.

We estimate the potential impact ι_{ab} of applying an import trade weight adjustment $W_{T\,ab}$ for a pair of countries a and b as the change in the amount available before and after the adjustment, averaged over all relevant products:

$$\iota_{ab} = W_{T\,ab} \cdot \langle T^i_{ab} \eta^{exp}_{a,i} {x_0}^i_a(0) \rangle_i \quad . \tag{4.1}$$

The results for the main rules are shown in table 4.2. In particular, relations between neighbouring countries intensify in the event of shocks, but size also matters. China, the world's second largest economy and second most populous country, shows the potential to gain huge additional trade volumes from other global players such as the United States. The highest multiplier does not imply the highest impact. For example, the `NLD - DEU` link has a higher impact than the `SYR - TUR` link, despite having a lower multiplier, because the initial trade value is much higher.

Only the adjustment for the import direction is discussed in more detail in the thesis. The export direction is not as interesting as the import direction due to the structure of the model. Once a country has allocated a certain amount of an item for export, it is irretrievably removed from the available amount and exported. Changing this allocation requires changing the allocation shares of η^{exp}, not the trade matrix itself. From our simplistic perspective, a country only cares about how much it exports, not how those exports are distributed around the world, as this does not increase the amount of product available within the country.

4.2.2 Most important product substitutions

We allow product substitution within the same commodity subgroup (see 5). There are 23 commodity subgroups, some of which contain up to 23 items, such as the subgroup *vegetables, fruits, nuts, legumes, spices*. However, there are also items that form their own subgroup and therefore have no potential substitutes, such as *Animal fats*, *Egg*, *Ethanol*, *Fish*, *Fodder crops*, *Grazing* or *Honey*. Within the group of primary products that are not directly or indirectly dependent on other product inputs in their production processes, [31], *Cereals* are the most relevant and we will explore the substitution rules for this group further. This subgroup includes products such as `Wheat and products`, `Maize and products`, `Rice and products`, etc., which are not only essential for food consumption but also play an important role in animal husbandry and therefore in the production of all kinds of animal products or in the production of other products such as sweeteners or beverages. The observed correlation between the shortage of an original product item and the increased import of a potential substitute item is shown in Figure 4.5. When a shortage of an item triggers the substitution step, the model increases all existing trade relationships for potential substitutes by the factor of the corresponding substitution index of the two products. Again, the trade share constraint will reduce the actual impact. The estimated impact of a substitution adjustment with S_{ij} is given by

$$\iota_{ij} = (1 + S_{ij}) \cdot \langle \sum_b T^j_{ab} \eta^{exp}_{a,j} x^j_a(0) \rangle_a \quad . \tag{4.2}$$

From the Table 4.3 we can see that maize and wheat are generally the most relevant substitutes for all other cereals, including each other. It lists the most important substitution relationships

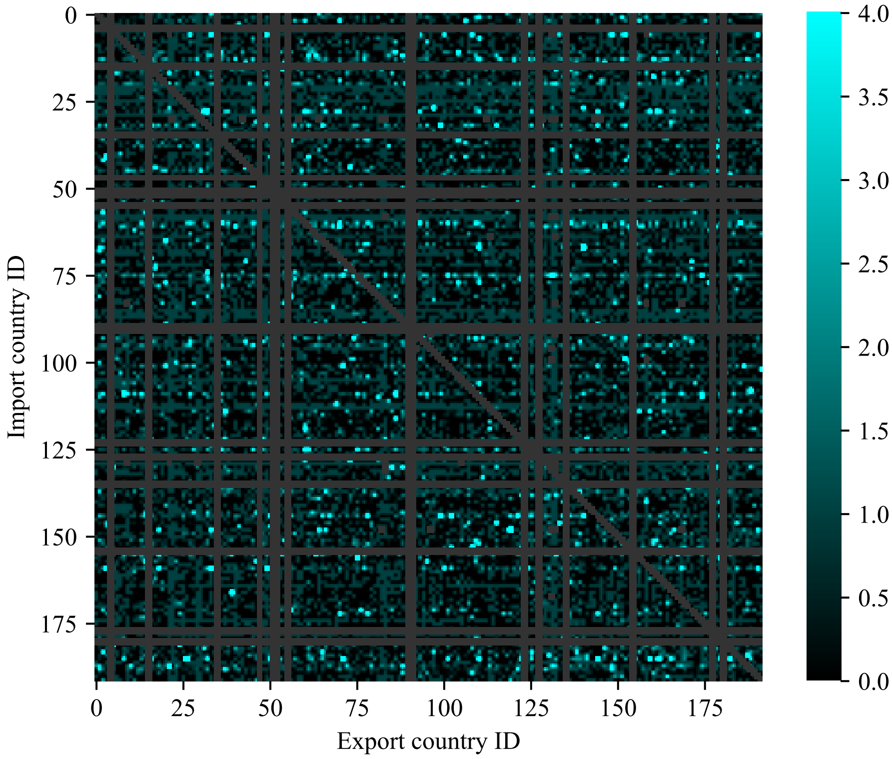

Figure 4.4: Import multiplier matrix $W_{T_{ab}}$. A value of 1, indicated by a dark cyan colour on the spectrum, represents no change in the multiplier for that parameter when the adjustment is triggered. Anything lighter indicates in increase when triggered. Dark grey areas indicate that this trade link between the two countries does not exist for any type of product. This mostly includes former nations that are still mentioned in the model due to their past existence between 1986 and 2020, but we have decided not to derive rules for them as an incomplete timeline would distort the event definition principles.

Table 4.3: Overview of impactful substitution rules within the commodity group *Cereals*. We show the top 10 most effective substitution rules. $S_{ij} + 1$ is the multiplier applied whenever a country experiences a shortage of food item i and increases its imports of item j as a substitute according to the estimated impact ι_{ij}.

Item	**Substitute item**	S_{ij}	**Estimated impact in ι_{ij} in 10^4 tons**
Rice and products	Wheat and products	0.127	13.04
Wheat and products	Maize and products	0.135	12.65
Maize and products	Wheat and products	0.104	10.61
Barley and products	Maize and products	0.110	10.36
Millet and products	Maize and products	0.095	8.93
Oats	Maize and products	0.092	8.59
Barley and products	Wheat and products	0.082	8.34
Rye and products	Maize and products	0.083	7.77
Oats	Wheat and products	0.069	7.11
Sorghum and products	Wheat and products	0.059	6.07

according to the substitution impact ι_{ij}. Among the top 10 relations, wheat and maize are the most frequent substitutes with substitution indices S_{ij} ranging from 0.081 to 0.127. Overall, there is a high degree of potential substitutability within the cereals sub-group, as shown in Figure 4.5, which shows the correlation coefficients. Each cereal has at least three possible substitutes and some are potentially substitutable by any other cereal, such as barley, oats, rice and wheat. The substitution indices range up to 0.2. Of the 72 possible substitution pairs, 53 show a significant correlation. In particular, barley, oats, rice and wheat seem to be easily substitutable, as we found substitution relationships with all other items in the cereals product group.

Given the potentially lower import volume of the substitute item in general, importing substitutes cannot fully compensate for all losses with a single product. However, the combination of importing several different items as substitutes can significantly mitigate losses. It is important to note that the availability of substitutes is not infinite, so full compensation for each shock may not be possible if a global shortage of one item leads to increased demand for similar items.

4.3 Adaptation in isolated shock scenarios

We have demonstrated the model by considering two isolated shock scenarios: a complete shock to Indian rice exports and to Ukrainian wheat exports. For both scenarios, we analyse two conditions: one in which the affected sectors can adapt by adjusting trade and production parameters (*India_adap* and *Ukraine_adap*), and one in which all parameters remain static throughout the simulation (*India_stat* and *Ukraine_stat*).

4.3.1 India's rice embargo

Background

Since 2022, India, the world's largest rice exporter, has imposed restrictions on grain exports, including a complete ban on non-basmati and broken white rice [41, 42]. Officially, the Indian government justifies the restrictions as necessary to protect domestic food security in the face of a growing population and the looming effects of climate change [41]. In response, global and domestic rice prices have risen significantly by double-digit percentage points over the past year, as India

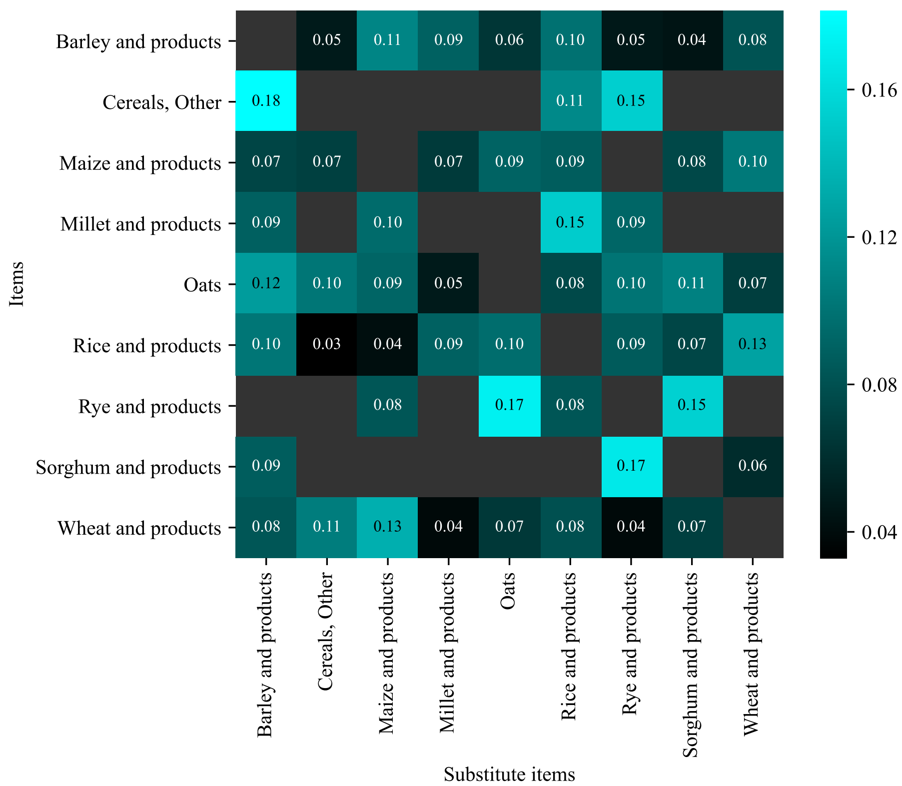

Figure 4.5: Substitution index matrix, S_{ij}, for the product group *Cereals*. The entries are the correlation coefficients between the decrease in availability (due to an event) of an item (row) and the increase in imports of its substitution cereal (column), derived according to 3.3.5. Missing values are indicated by a dark grey cell.

plays a significant role in the global rice trade, accounting for about 32.6% and a trade volume of 9.7 billion USD [41, 42].

Simulation results

The exogenous shock wipes out 100 % of India's rice production (a = `IND`, i = `Rice and products`), reducing India's rice exports to virtually zero. In the discussion of $L_{a\to b}^{i\to j}$, we will only focus on examining losses in countries other than India, although the models will also show large losses in India itself as this does not give a realistic picture of the situation from which the shock is derived, since the output that is virtually destroyed in the model is in reality still available for production processes in India and for consumption by the Indian population.

Figure 4.6 a) illustrates the uncompensated losses $L_{a\to b}^{i\to j}$ for the 50 most affected countries in *India_ stat* and the impact of adaptation with j = `Rice and products`. Djibouti (b = `DJI`) is the most affected country in both cases, with losses of up to 322.6 kg per person in *India_ adap*, exceeding the loss in *India_ stat*. Many of the worst-affected countries tend to fare worse in terms of the availability of rice itself, but some countries can reduce losses enormously. For example, the United Arab Emirates (b = `ARE`) reduces losses from 58.8 kg to 6.2 kg per person, Kuwait (b = `KWT`) reduces losses from 53.8 kg to 49.7 kg per person, and Oman (b = `OMN`) not only eliminates its losses but also manages to achieve a surplus of 11.3 kg per person compared to the unshocked baseline. Conversely, countries that experience significantly worse rice availability include Djibouti, Benin (b = `BEN`) (from 98.7 kg to 131.8 kg per person) and Timor-Leste (b = `TLS`) (from 65.4 kg to 155.6 kg per person). Each of these countries triggered the adjustment mechanism by experiencing high rice losses immediately at $t = 1$ due to their high dependence on India for rice imports. Both Djibouti and the United Arab Emirates import almost all of their rice, with India providing at least 75 % of their supply. The United Arab Emirates manages to make up some of the shortfall by sourcing additional rice from Vietnam or Thailand, while Djibouti is unable to find new suppliers within our framework. In Western Europe, where losses are small, most countries appear to benefit slightly, while other regions show mixed results. In fact, countries with a Human Development Index (HDI) below 0.6 [67] experience on average 4.8 % higher losses in the *India_ adap* scenario than in the *India_ stat* scenario, while countries with an HDI above 0.8 experience 14.2 % lower losses. Overall, compensatory efforts have only mitigated about 1 % of global rice losses, but about 30 % of the world's rice supply is irretrievably lost due to the shock. We can conclude that the compensatory efforts of countries do not necessarily lead to a reduction in losses. Overall, rice losses are mitigated by about 1 %. The main effect of adjustment is only redistributive. Given the constraints on economic growth, the system has to make do with what is available, making it impossible to fully mitigate shocks.

The simulations also show that the rice shock can be compensated to a considerable extent by substitution in several countries. More specifically, positive correlations were found for rice with all possible substitutes (see figure 4.5), while wheat is potentially the most effective substitution, see table 4.3. Appropriately, 4.7 a) shows increased j = `Wheat and products` availability for almost all to most countries affected by the Indian rice shock. Interestingly, countries seem to have adopted different strategies: While b = `ARE` try to import more of the shocked product themselves from their trading partners, others try to mitigate the losses by importing substitutes.

Looking at the impact of adjustments on secondary products, the shock to Indian rice shows little or no improvement, as rice can in principle be used as an input for the products mentioned in figure 4.8 a), but in reality rice is not as important as other cereals such as wheat or maize.

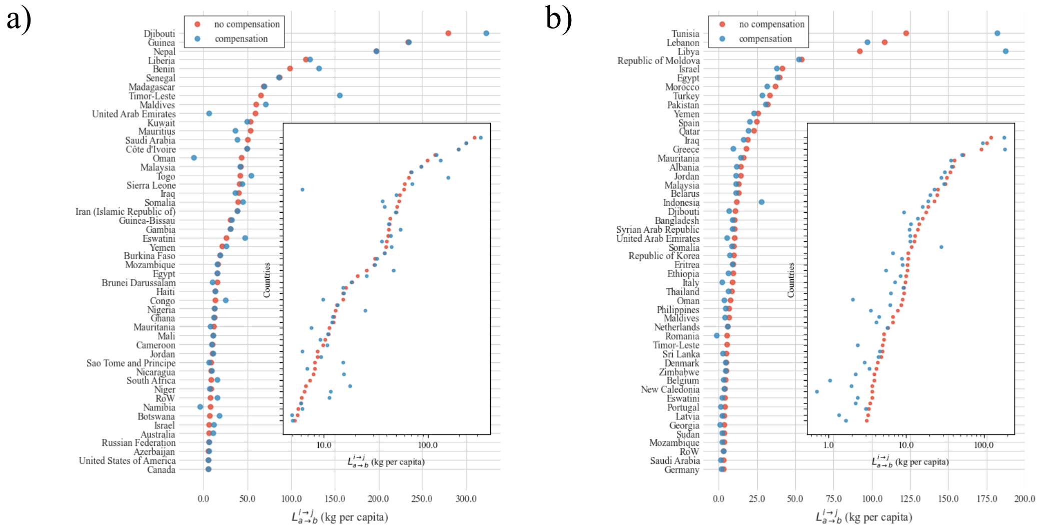

Figure 4.6: $L^{i\to j}_{a\to b}$ in the static (red) and adaptive (blue) scenarios for the top 50 losers in the static scenario: a) Shock to Indian rice (a = `IND`, i, j = `Rice and products`): Some of the worst-hit countries, such as the United Arab Emirates, Kuwait, Mauritius, Saudi Arabia and Oman, will be able to offset some of their losses. However, many others, such as Djibouti, Liberia, Benin, Timor-Leste or the Maldives, fare worse. On the linear scale, the less affected nodes appear to show little effect, but the logarithmic scale (inset) shows that the lower nodes are relatively similarly affected. b) Shock to Ukrainian wheat (a = `UKR`, i, j = `Wheat and products`): The most affected countries, with the exception of Tunisia, Libya or Indonesia, are able to reduce their losses through adapted strategies. Again, on the linear scale, the compensatory effect seems rather limited for the less affected nodes, but the logarithmic scale (inset) shows the relatively large gains at the lower end.

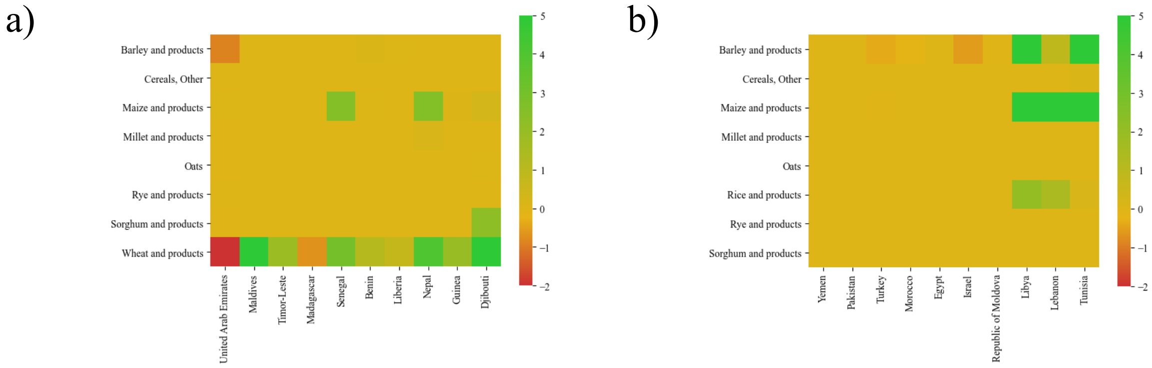

Figure 4.7: Adaptation impact $(L^{i\to j}_{a\to b})_{\text{stat}} - (L^{i\to j}_{a\to b})_{\text{adap}}$ in kg per capita on possible substitutes for the top 10 losers in the uncompensated scenario:
a) Indian rice shock (a = `IND`, i = `Rice and products`, $j = \{Cereals\}$): The most popular substitute is clearly wheat. Only in the United Arab Emirates is there no increase in its availability due to adaptation.
b) Ukrainian wheat shock (a = `IND`, i = `Wheat and products`, $j = \{Cereals\}$): The three countries initially most affected - Tunisia, Lebanon and Libya - import much more maize and barley.

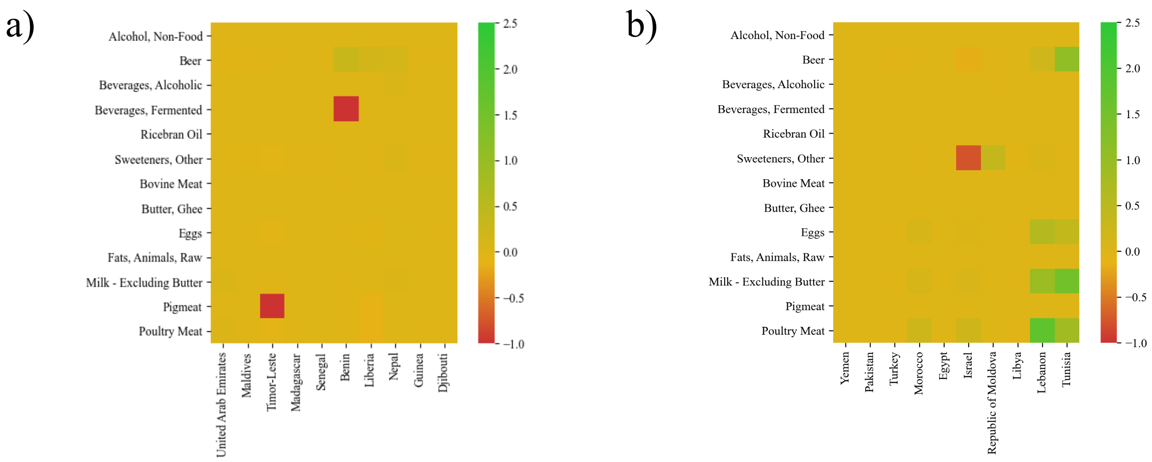

Figure 4.8: Adaptation impact $(L^{i\to j}_{a\to b})_{\text{stat}} - (L^{i\to j}_{a\to b})_{\text{adap}}$ in kg per capita on possible secondary products for the top 10 losers in the uncompensated scenario:
a) Indian rice shock (a = `IND`, i = `Rice and products`, $j = \{secondary\ items\}$): Rice is not as important as wheat as an input into production processes, and therefore losses in available secondary products are rather small and do not change significantly with adaptation, except for some singular losses in Liberia and Timor-Leste.
b) Shock to Ukrainian wheat (a = `UKR`, i = `Wheat and products`, $j = \{secondary\ items\}$): In particular, Tunisia and Lebanon improve their availability of j = `Poultry meat`, `Milk - excluding Butter`, `Eggs` and `Beer`, suggesting that the import of substitute items successfully supports efforts to mitigate losses.

4.3.2 Russian invasion of Ukraine and the Black Sea Grain Initiative

Background

Russia presented the world with another major threat to food security in February 2022 when it invaded Ukraine. The conflict has had serious political and economic consequences for both countries. Ukraine, a major producer of maize, wheat and sunflower oil, has suffered from the destruction of its infrastructure and the depletion of its labour force. The disruption of grain shipments through the Black Sea has exacerbated the 2022 global food price crisis [44]. With the July 2022 Black Sea Grain Initiative currently uncertain, exports remain vulnerable to Russian attacks [44].

Simulation results

We shock 100 % of Ukraine's wheat production ($a =$ `UKR`, $i =$ `Wheat and products`), which reduces Ukraine's wheat exports to zero. In the discussion of $L^{i \to j}_{a \to b}$, we will focus only on examining losses in countries other than Ukraine, although the models will also show large losses in Ukraine itself. This does not give a fully realistic picture of the situation from which the shock is derived, as the output that is almost completely destroyed in the model is in part still available for production processes in Ukraine and for consumption by the Ukrainian population in reality. In contrast to the Indian rice shock, where domestic production is unaffected by export restrictions, local production in Ukraine is heavily affected by the war and therefore does fall, but probably not as much as the complete elimination of all Ukrainian wheat production would suggest.

Figure 4.6 b) shows the wheat losses ($j =$ `Wheat and products`) for the top 50 most affected countries in *Ukraine_stat* for *Ukraine_adap* and *Ukraine_stat*. Tunisia ($b =$ `TUN`) emerges as the most affected country in *Ukraine_stat* with losses of 122.5 kg per capita, while Libya ($b =$ `LBY`) surpasses it in *Ukraine_adap* with losses of 187.5 kg per capita. Most of the severely affected countries tend to fare better in terms of wheat availability, but the situation in a few countries is deteriorating. Tunisia (rising to 181.9 kg per person) and Indonesia ($b =$ `IDN`) (rising from 11.8 kg to 28.0 kg per person) also experience worsening losses. On the other hand, Lebanon ($b =$ `LBN`) reduces its losses from 108.2 kg to 96.8 kg per person, Greece ($b =$ `GRC`) from 18.1 kg to 9.32 kg per person and Romania ($b =$ `ROU`) not only eliminates its losses but also achieves a surplus of 1.4 kg per person. Notably, wheat shortages are generally smaller than rice losses in the other shock simulation, and most countries fare better in *Ukraine_adap* than in *Ukraine_stat*. Not only is the shock to India's rice production almost ten times larger in absolute terms, but India's share of the world rice market (32.6%) is also about four times larger than Ukraine's share of the world wheat market (9.3%). The Indian rice shock leads to between 82 and 96% loss in rice supply for the top 10 most affected countries in the uncompensated scenario, while the Ukrainian wheat shock only leads to between 26 and 72% loss in wheat supply for the top 10 most affected countries in the uncompensated scenario.

According to table 4.5, maize shows the highest correlation as a potential substitute for wheat. Figure 4.8 b) shows that the availability of $b =$ `Maize and products` increases, especially in $b =$ `TUN`, `LBN` and `LBY`. Barley and, to a lesser extent, rice also appear to be popular substitutes for wheat. As Libya and Tunisia experience higher wheat losses with compensation, they appear to be trying to import alternative products, while other countries are trying to manage losses by importing wheat from other partners rather than increasing imports of other cereals. This again highlights the different strategies adopted by countries: While some try to import more of the shocked product itself, others try to mitigate losses by importing substitute products.

The impact of a Ukrainian wheat shock on secondary products is more pronounced than in the case of a shock to Indian rice. While these co-products can often be used in the same processes as inputs, including livestock, wheat is a much more popular input. Especially in $b =$ `TUN` and `LBN`, we see significant increases in the availability of j =`Poultry meat`, `Milk - excluding Butter`, `Eggs`, and `Beer`.

4.4 Superposition of shocks

So far we have only considered single shocks to the system. However, this approach can also be used to model the superposition of shocks. We want to investigate whether simultaneous shocks have a super-additive, sub-additive or no effect on losses. In particular, two large shocks to products within the same product subgroup can lead to interesting dynamics, as countries will try to mitigate the losses of both products by increasing imports of the same possible substitutes.

To assess the impact of two simultaneous shocks to sectors (a_1, i_1) and (a_2, i_2) on a recipient sector (b,j), we calculate the impact of the shock superposition $SI^{i_1,i_2\to j}_{a_1,a_2\to b}$. This allows us to conclude whether the shock superposition has a sub-additive, super-additive or no effect on the losses. This is done by comparing the combined losses from the superimposed scenario $L^{i_1,i_2\to j}_{a_1,a_2\to b}$ with the sum of the losses from the individual shock scenarios:

$$SI^{i_1,i_2\to j}_{a_1,a_2\to b} = L^{i_1,i_2\to j}_{a_1,a_2\to b} - (L^{i_1\to j}_{a_1\to b} + L^{i_2\to j}_{a_2\to b}) \quad . \tag{4.3}$$

If $SI^{i_1,i_2\to j}_{a_1,a_2\to b} > 0$, the losses indicate a super-additive shock effect, $SI^{i_1,i_2\to j}_{a_1,a_2\to b} < 0$ indicates a sub-additive effect.

(3.7) describe how the impact of a shock on sector (a, i) is felt in sector (b, j). Assessing the severity of the same shock to an entire region D with respect to food item j is done as follows:

$$L^{i\to j}_{a\to D}(t) = \frac{\sum\limits_{b\in D}\left(\underline{x}^j_b(t) - x^{i\to j}_{a\to b}(t)\right)}{\sum\limits_{b\in D} z_b} \tag{4.4}$$

If we want to assess the cumulative impact of a shock (a, i) on each product within a food group K in country b, the losses are calculated as follows:

$$L^{i\to K}_{a\to b}(t) = \frac{\sum\limits_{j\in K}\left(\underline{x}^j_b(t) - x^{i\to j}_{a\to b}(t)\right)}{z_b} \tag{4.5}$$

Combining both leads to:

$$L^{i\to K}_{a\to D}(t) = \frac{\sum\limits_{b\in D}\left(\sum\limits_{j\in K}\left(\underline{x}^j_b(t) - x^{i\to j}_{a\to b}(t)\right)\right)}{\sum\limits_{b\in D} z_b} \tag{4.6}$$

To determine the general impact of superposition of shocks on product groups or countries, we insert (4.6) into (4.3) and obtain the following formula for calculating the impact on group of countries D and group of products K:

$$SI^{i_1,i_2\to K}_{a_1,a_2\to D} = L^{i_1,i_2\to K}_{a_1,a_2\to D} - (L^{i_1\to K}_{a_1\to D} + L^{i_2\to K}_{a_2\to D}) \quad . \tag{4.7}$$

We now simulate the combined shocks of Indian rice (a_1 = `IND`, i_1 = `Rice and products`) and

Ukrainian wheat (a_2 = `UKR`, i_2 = `Wheat and products`) and compare the superposition impact $SI^{i_1,i_2\to j}_{a_1,a_2\to b}$ (4.3) for this scenario with and without adjustment.

Combined Shock Scenario Without Adaptation: In this scenario, we find that the losses are numerically identical to the sum of the isolated wheat and rice shocks for each recipient sector (b, j), so that the superposition effect is 0. This indicates that there is no interaction between the two shock propagation processes.

Combined Shock Scenario With Adaptation: When adaptive dynamics are considered, the results change. Focusing on the superposition impact $SI^{i_1,i_2\to K}_{a_1,a_2\to D}$ (4.7) on directly affected commodities globally as with $D = \mathcal{A}$ (all countries covered by the model) and $K =${`Rice and products, Wheat and products`}, the combined shocks have a sub-additive effect of $SI^{i_1,i_2\to K}_{a_1,a_2\to D}$, the combined shocks have a sub-additive effect of $SI^{i_1,i_2\to K}_{a_1,a_2\to D} = -0.05$ kg per capita, i.e. 0.05 kg more rice and wheat are available per person in the superimposed shock scenario.

However, when considering the impact of superposition on other food categories, the results are fundamentally different. Examining $SI^{i_1,i_2\to K}_{a_1,a_2\to D}$ (4.7) over the whole network with $D = \mathcal{A}$ and $K = \mathcal{I}$ (all items covered by the model), the result is $SI^{i_1,i_2\to K}_{a_1,a_2\to D} = 14.09$ kg per capita losses. There are super-additive effects. The 14.09 kg additional losses per capita represent about 0.1% of the average available volume per capita in relative terms.

The combined rice and wheat shocks are of particular interest because of their geopolitical relevance, as rice and wheat are direct substitutes. However, the question remains whether the subadditive effect on the shocked items and the superadditive effect on the whole network persists when other pairs of shocks are introduced, or whether it is just a special case of this particular pair. We therefore investigate the superposition effect of 1,000 superposed shocks, each randomly selecting two sectors (a_{r1}, i_{r1}) and (a_{r2}, i_{r2}), sampled from the 100 largest exporting primary product sectors by production volume. We compare their aggregated results $SI^{i_{r1},i_{r2}\to K}_{a_{r1},a_{r2}\to D}$ for the shocked products ($K = \{i_{r1}, i_{r2}\}$ and $D = \mathcal{A}$) and for the whole network ($K = \mathcal{I}$ and $D = \mathcal{A}$). Only shocks to sectors related to primary products and exports are eligible. Among the shocks that meet these criteria, we consider the largest 100 shocks according to their production volume. As a reference, Indian rice ranks 6 and Ukrainian wheat ranks 56 in the list according to this measure. Both products from the two shocks studied must always belong to the same product group in order for the superimposed substitution effect to take effect.

Superimposed Sampled Shock Scenarios With Adaptation: Similar to the case discussed above, the superimposed scenarios of the two random shocks show super-additive effects on the whole network. Fig. 4.9 a) shows the distribution of $SI^{i_{r1},i_{r2}\to K}_{a_{r1},a_{r2}\to D}$ with $D = \mathcal{A}$ and $K = \{i_{r1}, i_{r2}\}$, representing the global superposition effect in the products of the two shocked sectors. The distribution is centred around 0, with a mean $\langle SI^{i_{r1},i_{r2}\to K}_{a_{r1},a_{r2}\to D}\langle_{i_{r1},i_{r2}} = 0.09$ kg per capita. Figure. 4.9 b) shows the distribution of $SI^{i_{r1},i_{r2}\to K}_{a_{r1},a_{r2}\to D}$ with $D = \mathcal{A}$ and $K = \mathcal{I}$, representing the superposition effect over the whole network, with an average $\langle SI^{i_{r1},i_{r2}\to K}_{a_{r1},a_{r2}\to D}\langle_{i_{r1},i_{r2}} = 5.18$ kg per capita. The null hypothesis that the mean is 0 can be rejected with a p-value of 0.038, clearly indicating a super-additive effect of the superposition of shocks on the losses of the whole network.

Fig. 4.9 a) and 4.9 b) include insets showing scenarios with extreme outliers in additional or reduced losses due to superposition. One notable outlier is a simultaneous shock to soybeans from Brazil and the United States (grey arrow), resulting in $SI^{i_1,i_2\to K}_{a_1,a_2\to D} = -20$ kg per capita for soybeans and $SI^{i_1,i_2\to K}_{a_1,a_2\to D} = 1717$ kg per capita for all items. For comparison, a 20 kg per capita reduction in soybean losses corresponds to a relative gain of 40 %, and a 1717 kg per capita increase in losses across the network corresponds to an additional relative loss of 12 %.

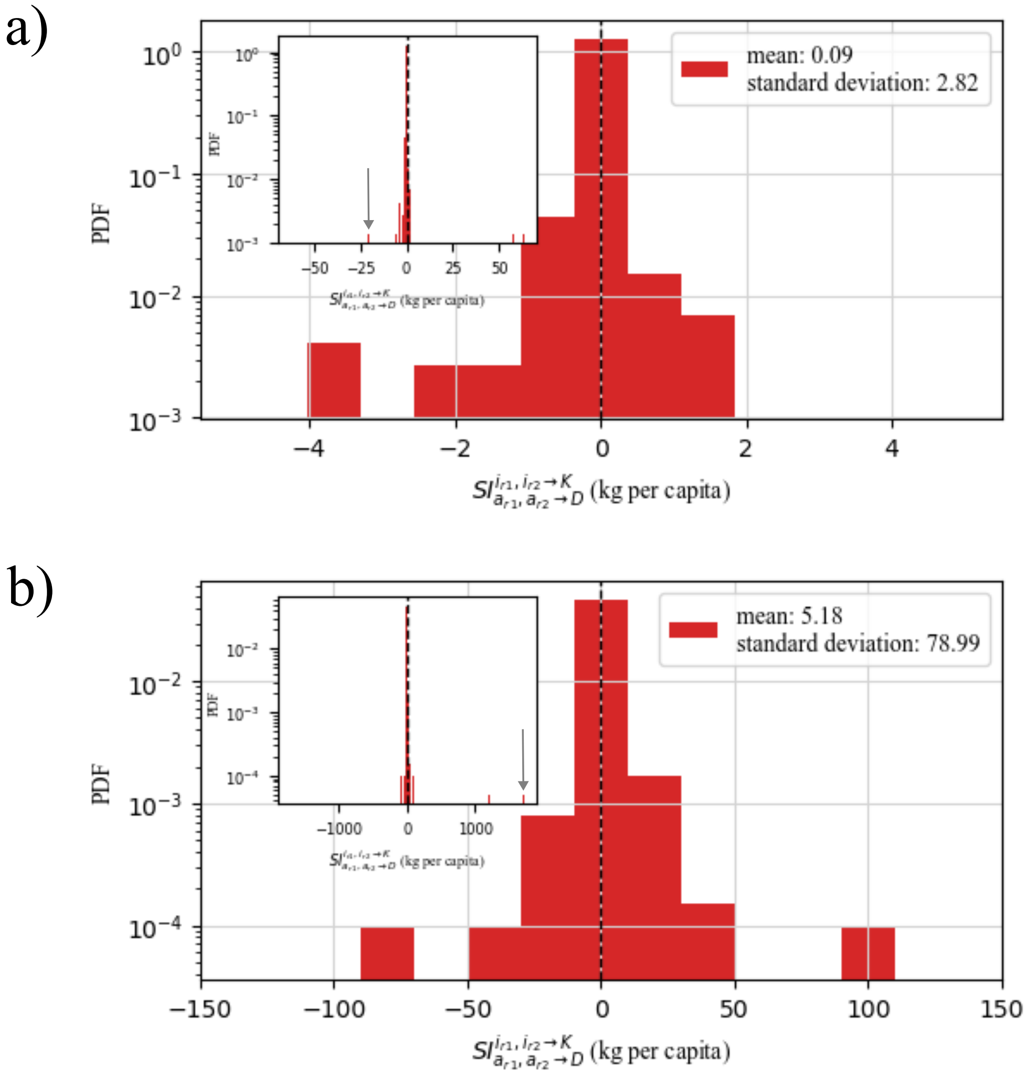

Figure 4.9: Histograms of $SI^{i_{r1},i_{r2}\to K}_{a_{r1},a_{r2}\to D}$ for sampled (a_{r1}, i_{r1}) and (a_{r2}, i_{r2}). The results are shown for (a) the shocked items ($D = \mathcal{A}$ and $K = \{i_{r1}, i_{r2}\}$) and (b) summed over all food items ($D = \mathcal{A}$ and $K = \mathcal{I}$) as probability density functions. Both distributions are centred around zero (black dotted line), with some outliers shown in the respective insets. The distribution of the effect on the shocked items themselves shows no evidence of sub- or super-additivity. However, the aggregated network effect indicates a slight super-additivity (p-value: 0.038). The grey arrow indicates an example of an extreme outlier in terms of super-additivity, a simultaneous shock to soybean production in the United States and Brazil.

5 Conclusion

We presented a method for modelling the macroscopic effects of exogenous food supply shocks by calibrating microscopic, data-driven, node-specific and validated adaptation rules. We apply these adaptation rules to the static shock propagation model of the global food production and trade network proposed by [31]. Here, the adaptation rules include strategies to cope with the incurred losses by adjusting their trade, production and allocation strategies for the affected sectors. In addition, countries can also adjust their trade strategy for sectors related to similar items that can serve as substitutes for the initially affected item.

The adjustment rules derived from historical events in the extensive food IO data [30] have been applied to the multilayer network model of food production and trade by [31]. A wide range of shock scenarios involving one or more agricultural products in one or more countries or regions can then be explored. The impact of compensatory efforts in response to shocks can be assessed, with a particular focus on the availability of resources. This impact is described in terms of absolute losses per capita, providing a versatile metric that not only indicates how severely a recipient sector is affected relative to others, but also highlights the intensity of the shock's impact on the population.

The effects of shock propagation in food supply networks can be modelled by taking inspiration from hysteresis, originally rooted in magnetism. The relevant properties of each system find equivalents in the other, as described in Section 2.1. The shock applied to the network represents an external influence to which the system is subjected. The resulting macroscopic outcome, such as the overall impact on the availability of agricultural goods, depends on the collective behaviour of microscopic equations of state. These equations are reinterpreted in this case as trade and production functions, with individual parameters assigned to each node of the network. As the shock propagates through the trade and production functions, the available quantities of goods are affected not only by their own initial quantities, but also by neighbouring nodes from which they import or use products as inputs in production, much as the spin states of a magnet are affected by the spin state of its surroundings. The relationship between the size of the shock and its impact cannot be described in simple linear terms; it depends on the nature and constitution of the shock. Allowing for the adaptation of the links, whether in terms of their strength or existence, does not negate this inherent property of the system, but rather enhances it. Adjustments affect not only the node that triggered them, but also other entities. For example, in the case of trade adjustments, where a country's export share for a particular item must add up to one, an increase in imports from one source country may lead to a decrease in imports from other exporters. The detailed procedure of deriving the microscopic adaptation was detailed in Chapter 3.

On the basis of $2,300$ relevant events, we have shown in Section 4.1 that stable and consistent trade and production adjustment strategies can indeed be derived from the data on a country and product-specific basis. In Section 4.2 we highlight some adjustment rules. In terms of trade adjustment, relations between neighbouring countries and major economic players appear to have the largest potential impact in absolute terms. The initial strength of the adjusted trade relationship proves to be very important, as a high multiplier does not necessarily lead to the highest additional trade volumes. Substitution, which we allow only for items in the same product group, is particularly relevant for cereals. Cereals are an important product group, as they are not only consumed directly, but are also used in many production processes.

The extended model is applied to case studies of isolated (4.3) and superimposed (4.4) shocks. First, we consider two shock scenarios: one affecting Indian rice production [41, 42] and one affecting Ukrainian wheat production [44, 43]. In *India_ adap*, compensation strategies were at least partially successful, mitigating agricultural losses in some areas but causing both negative and positive spillovers elsewhere. Globally, the loss of Indian rice could not be fully compensated, with only 1% of the losses being saved, highlighting the limitation of the strategy to simply reallocate the remaining available products. While potential secondary products are not severely affected, as rice is not as important as a production input compared to other cereals such as maize or wheat, we observe significant losses in rice availability, particularly in the Middle East and West Africa. The countries most affected by the shocks tend to have high import concentrations, making them highly vulnerable. Indian rice can account for up to 96 % of a country's rice imports. The compensation processes observed in response to reduced rice supplies disadvantage economically weaker countries. Countries with a low HDI experienced on average 4.8 % more losses after compensation compared to the uncompensated scenario, while countries with a very high HDI experienced 14.2 % less losses.

In the case of *Ukraine_ adap*, the compensatory trade and production adjustments resulted in much lower total wheat losses in the global food network, with almost all affected countries managing to increase wheat availability compared to *Ukraine_ stat*. Differences in the overall success of compensation strategies can be explained by the size of the shock relative to global supply and the degree of diversification of the importing countries. India's significant share of the world rice market means that some countries are highly dependent on imports from India. Conversely, the global supply of wheat is more diversified and countries are not as dependent on wheat imports from Ukraine. This difference in dependency and supply diversification is likely to contribute to the success of offset strategies in the Indian rice scenario compared to the Ukrainian wheat scenario. The impact on secondary products is more pronounced, as wheat is an important input in livestock production, along with maize and soybeans.

We then looked at how multiple simultaneous crises affect global food security by examining a hypothetical scenario of combined Ukrainian wheat and Indian rice shocks. Without adaptation, the impact of the combined shock was equal to the sum of the isolated impacts of the rice and wheat shocks. However, with adaptive capacity taken into account, we observed sub-additivity in losses for rice and wheat. We find super-additivity in losses when looking at the cumulative effect across all regions and food commodities. Sampling combined shocks yields a similar result for the superposition impact across the network. We find combinations of shocks that are particularly systemically risky, such as a simultaneous shock to soybeans in Brazil and the US. The superposition of these two shocks leads to highly exacerbated losses of an additional 12 % of available volume lost across all regions and food products.

These examples illustrate the impact of countries' compensatory efforts in response to shocks. In particular, the superposition of shocks, where trade and output parameters are kept static and countries are not allowed to adjust, leads to a relationship between shock size and impact. However, allowing countries to try to mitigate losses in the model reveals the non-linear relationship between shock size and impact, similar to magnetism, where the applied magnetic field and the magnetization of an object do not show a linear relationship, but we observe hysteresis and obtain the typical hysteresis curve (Figure 2.1). The inclusion of adaptation extends the non-linear effects of shocks from isolated to superimposed scenarios. Adaptation efforts can redistribute losses. In particular, in the case of shocks to commodities with large global market shares, adaptation efforts may not only mitigate losses for some recipients, but also exacerbate losses in initially less affected or even potentially unaffected regions. Shortages in the global food market can result not only from trade restrictions or armed conflict, but also from the consequences of climate change, such as droughts, floods, wildfires and food pests, or other extreme events that are becoming more likely [38].

The model has several limitations. First, it provides a simplified representation of an adaptive food supply network, allowing for isolated, limited adjustments in response to severe losses. The model is designed to adjust its parameters only twice, rather than continuously, in response to indirect subsequent losses. Furthermore, it does not allow switching between production processes, as this would require taking into account the capacity of production facilities [68], which is currently neglected.

Second, the model only considers linear production functions, whereas the implementation of Leontief production functions would provide a more comprehensive representation of actual production outputs and critical production inputs [69]. In addition, the model does not consider non-agricultural inputs or outputs, including critical inputs such as fertilisers [70], which play a crucial role in agricultural productivity.

Third, the model does not take into account the stocks that countries could draw on in the event of shocks and which could also be depleted [32, 71]. Currently, the amount of product available is derived solely from trade and production. Although some of the yield can be allocated to production, this effectively removes it from further use.

Fourth, the granularity of the model is limited by the resolution of the FABIO database. More detailed spatial data at the subnational level could provide deeper insights into which exact regions within a country are more affected by shocks [72]. In addition, the granularity of the product categories in the database presents challenges in accurately assessing the availability of specific food items [69]. For example, the category 'Wheat and products' includes not only wheat but also wheat-derived products such as flour, bread and pasta.

Fifth, shock propagation and adjustment mechanisms are modelled in the absence of prices and markets, which typically play a crucial role in supply dynamics [32, 20], as competition increases when the supply of a product decreases but demand remains constant.

Sixth and finally, the shocks considered are relatively simple compared to the complexity of the real world. For example, the Indian rice embargo only partially bans the export of certain types of rice, while imposing price barriers and export restrictions on others. The use of a complete shock to all rice production in India is a simplification and can be seen as a worst-case scenario.

Despite its limitations, this work significantly advances the understanding of how adaptation strategies can mitigate the impact of shocks on global food production systems. By integrating historical, sector-specific, data-driven adaptation rules into a multi-layer network model, we can make more accurate predictions of food availability following specific events. This approach provides a valuable framework for policymakers and researchers to develop more effective strategies for ensuring food security, especially in the face of multiple, simultaneous crises. Modelling the impact of food supply shocks by introducing microscopic trade and production functions and node-specific adjustment rules, inspired by hysteresis from magnetism and voter models, provides a viable option for studying global food security. By using tools from complexity and network science, we can uncover both the direct and indirect dependencies within the global supply chain and model the adaptive behaviour in response to shocks, consistent with the hysteresis metaphor. This improved understanding of the complex systemic risks inherent in global food trade and production can inform the development of more resilient supply chains.

Bibliography

[1] Stefan Thurner, Rudolf Hanel, and Peter Klimek. "1 Introduction to Complex Systems". In: *Introduction to the Theory of Complex Systems*. Oxford University Press, 2018. DOI: 10.1093/oso/9780198821939.003.0001.

[2] *The Nobel Prize in Physics 2021*. Oct. 2021. URL: https://www.nobelprize.org/prizes/physics/2021/summary/.

[3] Stuart Alan Kauffman. "Metabolic stability and epigenesis in randomly constructed genetic nets". In: *Journal of Theoretical Biology* 22.3 (1969), pp. 437–467. DOI: 10.1016/0022-5193(69)90015-0.

[4] Stuart A. Kauffmanm and Edward D. Weinberger. "The NK model of rugged fitness landscapes and its application to maturation of the immune response". In: *Journal of Theoretical Biology* 141.2 (1989), pp. 211–245. DOI: 10.1016/S0022-5193(89)80019-0.

[5] Vittoria Colizza et al. "The Role of the Airline Transportation Network in the Prediction and Predictability of Global Epidemics". In: *PNAS* 103.7 (2006), pp. 2015–2020. DOI: 10.1073/pnas.0510525103.

[6] Luís M.A Bettencourt et al. "Growth, innovation, scaling, and the pace of life in cities". In: *PNAS* 104.17 (2007), pp. 7301–7306. DOI: 10.1073/pnas.0610172104.

[7] Cesar A. Hidalgo and Ricardo Hausmann. "The Building Blocks of Economic Complexity". In: *PNAS* 106.26 (2009), pp. 10570–10575. DOI: 10.1073/pnas.0900943106.

[8] Matthieu Cristelli, Andrea Tacchella, and Luciano Pietronero. "The heterogeneous dynamics of economic complexity". In: *PLOS ONE* 10.2 (2015), e0117174–e0117174. DOI: 10.1371/journal.pone.0117174.

[9] Marco Bardoscia et al. "DebtRank: A Microscopic Foundation for Shock Propagation". In: *PLOS one* 10.6 (2015), e0130406–e0130406. DOI: 10.1371/journal.pone.0130406.

[10] Mária Ercsey-Ravasz et al. "Complexity of the international agro-food trade network and its impact on Food Safety". In: *PLOS ONE* 7.5 (2012), e37810. DOI: 10.1371/journal.pone.0037810.

[11] Megan Konar et al. "Scaling properties of food flow networks". In: *PLOS ONE* 13.7 (2018), e0199498. DOI: 10.1371/journal.pone.0199498.

[12] Birgit Müller et al. "Modelling food security: Bridging the gap between the micro and the macro scale". In: *Global Environmental Change* 63 (2020), p. 102085. DOI: 10.1016/j.gloenvcha.2020.102085.

[13] Ken Dozier and David Chang. "A Physics Approach to Supply Chain Oscillations and Their Control". In: *Supply Chain the Way to Flat Organisation*. IntechOpen, 2009. Chap. 9. DOI: 10.5772/6658.

[14] Thibaut Cerabona et al. "Physics of decision: Managing and preparing critical supply chains to supply disruptions". In: *IFAC-PapersOnLine* 56.2 (2023), pp. 11135–11140. DOI: 10.1016/j.ifacol.2023.10.830.

[15] Thibaut Cerabona et al. "A Physics-Based Approach for Managing Supply Chain Risks and Opportunities Within Its Performance Framework". In: *Boosting Collaborative Networks 4.0*. Springer International Publishing, 2020, pp. 418–427. DOI: 10.1007/978-3-030-62412-5_34.

[16] Dirk Helbing et al. "Physics, stability, and dynamics of Supply Networks". In: *Physical Review E* 70.6 (2004), p. 066116. DOI: 10.1103/PhysRevE.70.066116.

[17] Dirk Helbing. "Modelling supply networks and business cycles as unstable transport phenomena". In: *New Journal of Physics* 5.1 (2003), p. 90. DOI: 10.1088/1367-2630/5/1/390.

[18] Takashi Nagatani and Dirk Helbing. "Stability analysis and stabilization strategies for linear supply chains". In: *Physica A: Statistical Mechanics and its Applications* 335.3 (2004), pp. 644–660. DOI: 10.1016/j.physa.2003.12.020.

[19] Tiziano Distefano et al. "Shock transmission in the International Food Trade Network". In: *PLOS ONE* 13.8 (Aug. 2018), pp. 1–15. DOI: 10.1371/journal.pone.0200639.

[20] Christopher Bren d'Amour et al. "Teleconnected food supply shocks". In: *Environmental Research Letters* 11.3 (Feb. 2016), p. 035007. DOI: 10.1088/1748-9326/11/3/035007.

[21] Richard S. Cottrell et al. "Food production shocks across land and sea". In: *Nature News* (Jan. 2019), pp. 130–137. DOI: https://doi.org/10.1038/s41893-018-0210-1.

[22] Jacob Schewe, Christian Otto, and Katja Frieler. "The role of storage dynamics in annual wheat prices". In: *Environmental Research Letters* 12.5 (Apr. 2017), p. 054005. DOI: 10.1088/1748-9326/aa678e.

[23] Derek Headey. "Rethinking the global food crisis: The role of trade shocks". In: *Food Policy* 36.2 (2011), pp. 136–146. DOI: 10.1016/j.foodpol.2010.10.003.

[24] Marco Lagi et al. "The Food Crises: A quantitative model of food prices including speculators and ethanol conversion". In: *SSRN Electronic Journal* (2011). DOI: 10.2139/ssrn.1932247.

[25] Getaw Tadesse et al. "Drivers and triggers of international food price spikes and volatility". In: *Food Policy* 47 (2014), pp. 117–128. DOI: 10.1016/j.foodpol.2013.08.014.

[26] Jessica A Gephart et al. "Vulnerability to shocks in the global seafood trade network". In: *Environmental Research Letters* 11.3 (Feb. 2016), p. 035008. DOI: 10.1088/1748-9326/11/3/035008.

[27] Rebekka Burkholz and Frank Schweitzer. "International crop trade networks: the impact of shocks and cascades". In: *Environmental Research Letters* 14.11 (Oct. 2019), p. 114013. DOI: 10.1088/1748-9326/ab4864.

[28] Marie-Cécile Dupas, José Halloy, and Petros Chatzimpiros. "Time dynamics and invariant subnetwork structures in the world cereals trade network". In: *PLOS ONE* 14.5 (May 2019), pp. 1–21. DOI: 10.1371/journal.pone.0216318.

[29] Kathyrn R. Fair, Chris T. Bauch, and Madhur Anand. "Dynamics of the Global Wheat Trade Network and Resilience to Shocks". In: *Scientific Reports* 7.1 (Aug. 2017), p. 7177. DOI: 10.1038/s41598-017-07202-y.

[30] Martin Bruckner et al. "Fabio—the construction of the Food and agriculture biomass input–output model". In: *Environ. Sci. Technol.* 53.19 (2019), pp. 11302–11312. DOI: 10.1021/acs.est.9b03554.

[31] Moritz Laber et al. "Shock propagation from the Russia–Ukraine conflict on International Multilayer Food Production Network Determines Global Food Availability". In: *Nature Food* 4.6 (2023), pp. 508–517. DOI: 10.1038/s43016-023-00771-4.

[32] Philippe Marchand et al. "Reserves and trade jointly determine exposure to food supply shocks". In: *Environmental Research Letters* 11.9 (Sept. 2016), p. 095009. DOI: 10.1088/1748-9326/11/9/095009.

[33] Ronald E. Miller and Peter D. Blair. *Input-Output Analysis: Foundations and Extensions*. 2nd ed. Cambridge University Press, 2009.

[34] Luca Galbusera and Georgios Giannopoulos. “On input-output economic models in disaster impact assessment”. In: *International Journal of Disaster Risk Reduction* 30 (2018), pp. 186–198. DOI: 10.1016/j.ijdrr.2018.04.030.

[35] *The State of Agricultural Commodity Markets 2022. The geography of food and agricultural trade:Policy approaches for sustainable development*. 2022. DOI: 10.4060/cc0471en.

[36] Michael J Puma et al. “Assessing the evolving fragility of the global food system”. In: *Environmental Research Letters* 10.2 (Feb. 2015), p. 024007. DOI: 10.1088/1748-9326/10/2/024007.

[37] Anuradha Mittal. “The 2008 Food Price Crisis: Rethinking Food Security Policies”. In: *G-24 Discussion Paper Series* 56 (2009).

[38] Kyle Frankel Davis, Shauna Downs, and Jessica A. Gephart. “Towards Food Supply Chain Resilience to environmental shocks”. In: *Nature Food* 2.1 (2020), pp. 54–65. DOI: 10.1038/s43016-020-00196-3.

[39] Leonie Wenz and Anders Levermann. “Enhanced economic connectivity to foster heat stress–related losses”. In: *Science Advances* 2.6 (2016), e1501026. DOI: 10.1126/sciadv.1501026.

[40] Richard A. Holley and Thomas M. Liggett. “Ergodic Theorems for Weakly Interacting Infinite Systems and the Voter Model”. In: *The Annals of Probability* 3.4 (1975), pp. 643–663. DOI: 10.1214/AOP/1176996306.

[41] Benjamin Parkin et al. “The return of the rice crisis”. In: *Financial Times* (Oct. 2023). URL: https://www.ft.com/content/416736ec-7960-496d-b6c8-fd7a2fd99668.

[42] *Global Information and Early Warning System Country Briefs India*. 2023. URL: https://www.fao.org/giews/countrybrief/country.jsp%3Fcode=IND.

[43] *United Nations Two-Year Update - Protection of civilians: impact of hostilities on civilians since 24 February 2022*. 2024. URL: https://www.ohchr.org/en/documents/country-reports/two-year-update-protection-civilians-impact-hostilities-civilians-24.

[44] *Brief on the interruption of the Black Sea Grain Initiative and its potential implications on global food markets and food security*. 2023. URL: https://openknowledge.fao.org/handle/20.500.14283/cc7271en.

[45] Carl Friedrich Gauss. “Theoria attractionis Corporum Sphaeroidicorum ellipticorum homogeneorum, Methodo Nova tractata”. In: *Werke* (1877). DOI: 10.1007/978-3-642-49319-5_8.

[46] Charles-Augustin de Coulomb. “Premier mémoire sur l’électricité et le magnétisme”. In: *Histoire de l’Académie Royale des Sciences* (1785). DOI: 10.5479/sil.304245.39088000647479.

[47] Isaac Newton. *Philosophiae Naturalis Principia Mathematica*. 1687. DOI: 10.5479/sil.52126.39088015628399.

[48] Sōshin Chikazumi and C D Graham Jr. “Magnetostatic Phenomena”. In: *Physics of Ferromagnetism*. Oxford University Press, 1997. DOI: 10.1093/oso/9780198517764.003.0001.

[49] James Alfred Ewing. “On the production of transient electric currents in iron and steel conductors by twisting them when magnetised, or by magnetising them when twisted”. In: *Proceedings of the Royal Society of London* 36.228-231 (1883), pp. 117–135. DOI: 10.1098/rspl.1883.0084.

[50] Richard P. Feynman, Robert B. Leighton, and Matthew Sands. “Magnetic Materials”. In: *The Feynman Lectures on Physics*. Vol. 2. Addison-Wesley, 1964. Chap. 37.

[51] Rod Cross. “On the Foundations of Hysteresis in Economic Systems”. In: *Economics and Philosophy* 9.1 (1993), pp. 53–74. DOI: 10.1017/S0266267100005113.

[52] Ernst Ising. “Beitrag zur Theorie des Ferromagnetismus”. In: *Zeitschrift für Physik* 31 (1925), pp. 253–258. DOI: 10.1007/BF02980577.

[53] Lars Onsager. “Crystal Statistics. I. A Two-Dimensional Model with an Order-Disorder Transition”. In: *Phys. Rev.* 65 (3-4 1944), pp. 117–149. DOI: 10.1103/PhysRev.65.117.

[54] James P. Gleeson. "Binary-State Dynamics on Complex Networks: Pair Approximation and Beyond". In: *Phys. Rev. X* 3 (2 2013), p. 021004. DOI: 10.1103/PhysRevX.3.021004.

[55] Arkadiusz Jędrzejewski and Katarzyna Sznajd-Weron. "Statistical Physics Of Opinion Formation: Is it a SPOOF?" In: *Comptes Rendus Physique* 20.4 (2019), pp. 244–261. DOI: 10.1016/j.crhy.2019.05.002.

[56] Sidney Redner. "Reality-inspired voter models: A mini-review". In: *Phys. Rev. E* 80 (4 2009), p. 041129. DOI: 10.1103/PhysRevE.80.041129.

[57] Jinming Du. "Voter model on adaptive networks". In: *Chinese Physics B* 31.5 (2022), p. 058902. DOI: 10.1088/1674-1056/ac43b4.

[58] Adriaan Fokker. "Die mittlere Energie rotierender elektrischer Dipole im Strahlungsfeld". In: *Annalen der Physik* 348 (1914), pp. 810–820. DOI: 10.1002/andp.19143480507.

[59] Max Planck. "Über einen Satz der statistischen Dynamik und seine Erweiterung in der Quantentheorie". In: *Sitzungsberichte der Preussischen Akademie der Wissenschaften zu Berlin* 24 (1917), pp. 324–241.

[60] Claudio Castellano, Miguel A. Muñoz, and Romualdo Pastor-Satorras. "Nonlinear q-voter model". In: *Comptes Rendus Physique* 20 (4 2019), pp. 275–292. DOI: 10.1016/j.crhy.2019.05.004.

[61] Henry Wai-chung Yeung and Neil Coe. "Toward a Dynamic Theory of Global Production Networks". In: *Economic Geography* 91.1 (2015), pp. 29–58. DOI: 10.1111/ecge.12063.

[62] Tomasz Raducha and Maxi San Miguel. "Emergence of complex structures from nonlinear interactions and noise in coevolving networks". In: *Scientific Reports* 10 (1 2020), p. 15660. DOI: 10.1038/s41598-020-72662-8.

[63] "World Population Prospects 2022". In: *United Nations, Department of Economic and Social Affairs, Population Division* (2022). URL: https://population.un.org/wpp/Download/Standard/MostUsed/.

[64] Jill E. Hobbs. "Food supply chain resilience and the COVID-19 pandemic: What have we learned?" In: *Canadian Journal of Agricultural Economics/Revue canadienne d'agroeconomie* 69.2 (2021), pp. 189–196. DOI: 10.1111/cjag.12279.

[65] Yoav Benjamini and Yosef Hochberg. "Controlling the False Discovery Rate: A Practical and Powerful Approach to Multiple Testing". In: *Journal of the Royal Statistical Society: Series B (Methodological)* 57.1 (1995), pp. 289–300. DOI: 10.1111/j.2517-6161.1995.tb02031.x.

[66] Brain W. Matthews. "Comparison of the predicted and observed secondary structure of T4 phage lysozyme". In: *Biochimica et Biophysica Acta (BBA) - Protein Structure* 405.2 (1975), pp. 442–451. DOI: 10.1016/0005-2795(75)90109-9.

[67] "Human Development Report 2021-22". In: *UNDP (United Nations Development Programme)* (2022). URL: http://report.hdr.undp.org.

[68] Jukka Korpela et al. "An analytic approach to production capacity allocation and supply chain design". In: *International Journal of Production Economics* 78.2 (2002), pp. 187–195. DOI: https://doi.org/10.1016/S0925-5273(01)00101-3.

[69] Christian Diem et al. "Quantifying firm-level economic systemic risk from nation-wide supply networks". In: *Scientific Reports* 12.1 (2022), p. 7719. DOI: 10.1038/s41598-022-11522-z.

[70] Michael Obersteiner et al. "The phosphorus trilemma". In: *Nature Geoscience* 12.1 (2013), pp. 897–898. DOI: 10.1038/ngeo1990.

[71] Richard Oloruntoba, Ramaswami Sridharan, and Graydon Davison. "A proposed framework of key activities and processes in the preparedness and recovery phases of disaster management". In: *Disasters* 42.3 (2018), pp. 541–570. DOI: https://doi.org/10.1111/disa.12268.

[72] Asjad Naqvi, Franziska Gaupp, and Stefan Hochrainer-Stigler. "The risk and consequences of multiple breadbasket failures: an integrated copula and multilayer agent-based modeling approach". In: *OR Spectrum* 42.3 (Sept. 2020), pp. 727–754. DOI: 10.1007/s00291-020-00574-0.

Supplementary Information

Data reconciliation and validation

To validate the simulation results, a comparison with real data would be ideal. Unfortunately, we lack specific data describing the effects of singular shock propagation or its compensation mechanisms, apart from our base dataset, FABIO [30]. We therefore make use of this available dataset and the resulting parameters, which include a starting vector ${x_0}^i_a$ for each year. Instead of deriving parameters from the usual 29 years (1992 to 2020), we base the adjustment rules on the first 19 years (1992 to 2010) and use the remaining years (2011 to 2020) as a benchmark. The benchmark vectors, consisting of the initial vectors ${x_0}^i_a$, are normalised with respect to the first year included in the benchmark, 2011, similar to the equation (3.10) but using 2011 instead of 1992.

For the simulation scenarios, we calculate the baseline scenario as usual, using the model parameters derived from the data for 2011. For the two shocked scenarios (no compensation and compensation), the initiated shock consists of the real events of 2011 observed in the data. Any event in 2011 that meets the criteria of a relative loss greater than 0.26, an absolute loss greater than 1000 tonnes and a maximum deviation of 0.32 before and after the event is considered. According to the obtained set of shock events (a, i, l) for the affected item i in area a with a relative loss of l, the reduced production outputs are derived using the equation (3.6), where l replaces ϕ. Production is reduced at each time step t of the simulation as follows:

$$o^i_a(t) = (1 - l^i_a) \cdot o^i_a(t) \quad \forall t \in \{0, ..., \tau\} \quad . \tag{5.1}$$

The static scenario is run as described in section 3.2 using the model parameters derived from the 2011 data and the events described above. In addition, the adaptive scenario applies the adjustment rules as described in sections 3.3.4 and 3.3.5. The results are shown in figures 5.1 and 5.2. The market share of a sector is (a, i):

$$s^i_a(t) = \frac{x^i_a(t)}{\sum\limits_{a \in \mathcal{A}} x^i_a(t)} \quad . \tag{5.2}$$

Comparing the average market share $\langle s^i_a(t) \langle_t$ of a country for an item over the simulation period and its standard deviation $\sigma_{s^i_a(t)}$, it can be seen that the scenario allowing for adjustment models the fluctuations in available quantity more realistically than the static model. However, the trend in the standard deviation $\sigma_{x^i_a(t)}$ of the per capita volume of an item in a region over the simulation period is inconclusive. The baseline and the two shock scenarios show significantly lower dispersion than the benchmark scenario, but they cannot be properly distinguished from each other. Both the $\langle s^i_a(t) \rangle_t$ and the $\langle x^i_a(t) \rangle_t$ time series roughly follow the distribution of the benchmark scenario.

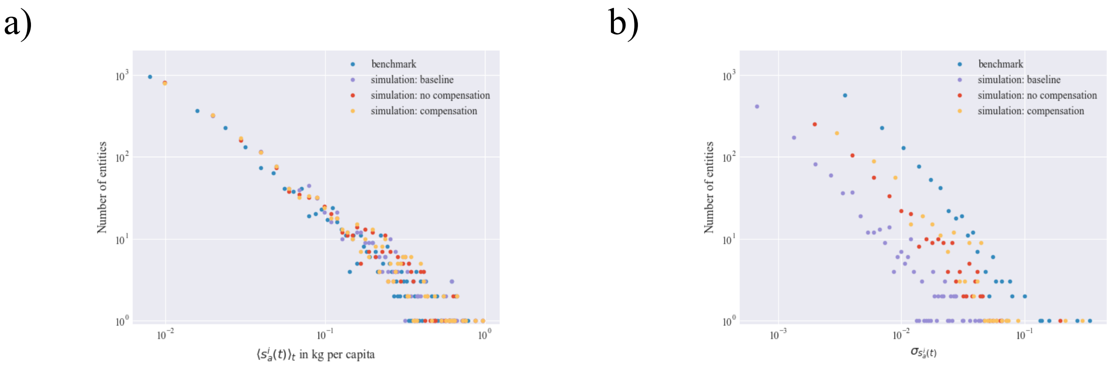

Figure 5.1: Comparison of (a) a country's mean market share $\langle s_a^i(t)\rangle_t$ of an item over the duration of the simulation and (b) $\sigma_{s_a^i(t)}$. The mean shows similar distributions for all three simulations included in the graph (purple: baseline, red: no compensation or static, yellow: compensation or adaptive), which in turn are very similar to the benchmark (blue). As for the standard deviation, the values for the benchmark scenario are much higher than for the baseline or shock simulation. The compensation scenario has the highest standard deviations among the simulation scenarios and is therefore closest to the benchmark.

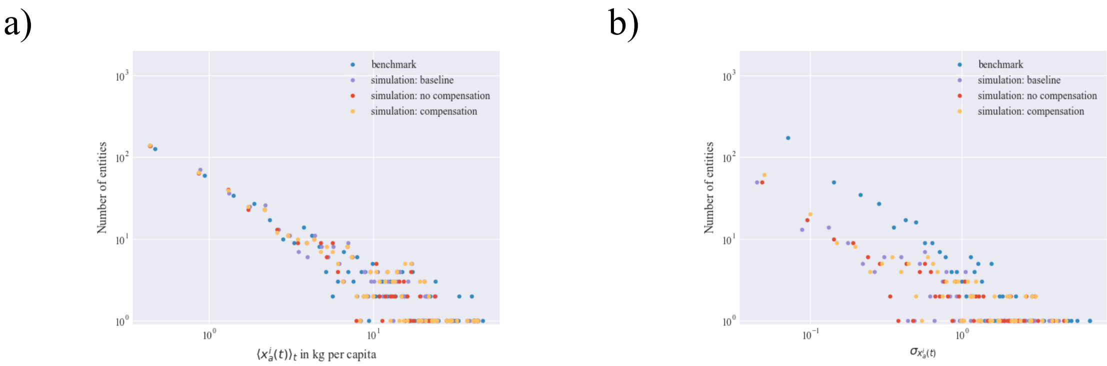

Figure 5.2: Comparison of (a) the mean available volume per capita $\langle x_a^i(t)\rangle_t$ in a sector (a, i) over the duration of the simulation and (b) its standard deviation $\sigma_{x_a^i(t)}$. The mean again shows similar distributions for all three simulations included in the graph (purple: baseline, red: no compensation or static, yellow: compensation or adaptive), which are again very similar to the benchmark (blue). As for the standard deviation, the values for the simulations follow similar distributions, each with values significantly lower than the benchmark and not really distinguishable from each other.

List of food items and commodity groups

Table 5.1: Products and their respective product subgroup and product group. Products within the same product subgroup are considered as possible substitutes in 3.3.5

Product group	Product subgroup	Product
Crop products	Alcohol	Beer Beverages, Alcoholic Beverages, Fermented Wine
	Ethanol	Alcohol, Non-food
	Fibre crops	Cotton lint Cottonseed
	Oil cakes	Copra Cake Cottonseed Cake Groudnut Cake Oilseed Cakes, other Palmkernel, Cake Rape and Mustard Cake Sesameseed Cake Soyabean Cake Sunflowerseed Cake
	Oil crops	Palm kernels
	Sugar, sweeteners	Sugar (raw equivalent) Sugar non-centrifugal Sweeteners, other
	Vegetable oils	Coconut Oil Cottonseed Oil Groundnut Oil Maize Germ Oil Oilcrops Oil, other Olive Oil Palm Oil Palmkernel Oil Rape and Mustard Oil Ricebran Oil Sesamesees Oil Soyabean Oil Sunflowerseed Oil
Fish	Fish	Fish, Seafood
Livestock	Live animals	Asses Buffaloes Camelids, other Cattle Goats Horses Mules Pigs Poultry Birds Rabbits and hares Rodents, other

Livestock	Live animals	Sheep
Livestock products	Animal fats	Fats, Animal, Raw
	Eggs	Eggs
	Hides, skins, wool	Hides and skins Silk Wool (clean equivalent)
	Honey	Honey
	Meat	Bovine Meat Meat, other Mutton & Goat Meat Offals, edible Pigmeat Poulty Meat
Primary crops	Cereals	Barley and products Cereals, other Maize and products Millet and products Oats Rice and products Rye and products Sorghum and products Wheat and products
	Coffee, tea, cocoa	Cocoa Beans and products Coffee and products Tea (including mate)
	Fibre crops	Abaca Hard Fibres, other Jute Jute-Like Fibres Sisal Soft-Fibres, other
	Fodder crops	Fodder crops
	Grazing	Grazing
	Oil crops	Coconuts (including Copra) Groundnuts Oil, palm fruit Oilcrops, other Olives (including preserved) Rape and Mustardseed Seed cotton Sesame seed Soyabeans Sunflower seed
	Roots and tubers	Cassava and products Potatoes and products Roots, other Sweet potatoes Yams
	Sugar crops	Sugar beet Sugar cane
	Tabacco, Rubber	Rubber Tobacco

Primary crops	Vegetables, fruit, nuts, pulses, spices	Apples and products Bananas Beans Citrus, other Cloves Dates Fruits, other Grapefruit and products Grapes and products (excluding Wine) Hops Lemons, Limes and products Nuts and products Onions Oranges, Mandarines Peas Pepper Pimento Pineapples and products Plantains Pulses, other and products Spices, other Tomatoes and products Vegetables, other

List of countries

Table 5.2: Countries and their respective region. The table also lists countries, that do not exist anymore, but only ceased to exist after 1986.

Continent	Region	Country
Africa	Africa N	Algeria
		Egypt
		Libya
		Morocco
		Sudan
		Tunisia
	Africa S	Angola
		Benin
		Botswana
		Burkina Faso
		Burundi
		Cabo Verde
		Cameroon
		Central African Republic
		Chad
		Côte d'Ivoire
		Congo
		Democratic Republic of the Congo
		Djibouti
		Eritrea
		Eswatini
		Ethiopia
		Gabon
		Ghana
		Guinea
		Guinea-Bissau
		Kenya
		Lesotho
		Liberia
		Madagascar
		Malawi
		Mali
		Mauritania
		Mauritius
		Mozambique
		Namibia
		Niger
		Nigeria
		Rwanda
		Sao Tome and Principe
		Senegal
		Sierra Leone
		Somalia
		South Africa
		South Sudan
		Sudan

Africa	Africa S	Togo United Republic of Tanzania Uganda Zambia Zimbabwe
Asia	Asia C	Kazakhstan Kyrgyzstan Tajikistan Turkmenistan Uzbekistan
	Asia E	China, Hong Kong SAR China, Macao SAR China, mainland China, Taiwan Province Democratic People's Republic of Korea Japan Mongolia Republic of Korea
	Asia N	USSR
	Asia S	Afghanistan Bangladesh India Iran (Islamic Republic of) Maldives Nepal Pakistan Sri Lanka
	Asia SE	Brunei Darussalam Cambodia Indonesia Malaysia Myanmar Lao People's Democratic Republic Philippines Singapore Thailand Timor-Leste Viet Nam
	Asia W	Armenia Azerbaijan Bahrain Cyprus Georgia Iraq Israel Jordan Kuwait Lebanon Oman Qatar Saudi Arabia Syrian Arab Republic

Asia	Asia W	Turkey United Arab Emirates Yemen
Europe	Europe E	Belarus Bulgaria Czech Republic Czechoslovakia Hungary Poland Republic of Moldova Romania Russian Federation Slovakia Ukraine
	Europe N	Denmark Estonia Finland Iceland Ireland Latvia Lithuania Norway Sweden United Kingdom
	Europe S	Albania Bosnia and Herzegovina Croatia Greece Italy Malta Montenegro North Macedonia Portugal Serbia Serbia and Montenegro Slovenia Spain Yugoslav SFR
	Europe W	Austria Belgium Belgium-Luxembourg France Germany Luxembourg Netherlands Switzerlands
Oceania	Australia	Australia New Zealand
	Melanesia	Fiji New Caledonia Papua New Guinea Solomon Islands

Oceania	Melanesia	Vanuatu
	Micronesia	Kiribati
	Polynesia	French Polynesia Samoa
North America	America N	Canada United States of America
South America	America S	Antigua and Barbuda Argentina Bahamas Barbados Belize Bolivia (Plurinational State of) Bolivarian Republic of Venezuela Brazil Chile Colombia Costa Rica Cuba Dominica Dominican Republic Ecuador El Salvador Grenada Guatemala Guyana Haiti Honduras
	America Latin and Caribbean	Jamaica Mexico Netherlands Antilles Nicaragua Panama Paraguay Peru Puerto Rice Saint Kitts and Nevis Saint Lucia Saint Vincent and the Grenadines Suriname Trinidad and Tobago Uruguay
not classified	not classified	RoW

List of processes

Table 5.3: Processes divided in primary production and processing

Process type	Process
Primary production	Abaca production Apples production Asses husbandry Bananas production Barley production Beans production Buffaloes husbandry Camelids husbandry, other Camels husbandry Cassava production Cattle husbandry Cereals production, other Citrus production, other Cloves production Cocoa Beans production Coconuts production Coffee production Dairy buffaloes husbandry Dairy camels husbandry Dairy cattle husbandry Dairy goats husbandry Dairy sheep husbandry Dates production Fishing Fodder crops production Fruits production, other Goats husbandry Grapefruit production Grapes production Grazing production Groundnut (shelled equivalent) production Hard Fibres production, other Hops production Horses husbandry Jute production Jute-Like Fibres production Lemons,Limes production Maize production Millet production Mules husbandry Nuts production Oat production Oil palm fruit production Oilcrops production, other Olives production Onions production

Primary production	Oranges, Mandarines production
	Peas production
	Pepper production
	Pigs farming
	Pimento production
	Pineapples production
	Plantains production
	Potatoes production
	Poultry Birds farming
	Pulses production, other
	Rabbits husbandry
	Rape and Mustardseed production
	Rice production
	Rodents husbandry, other
	Roots production, other
	Rubber production
	Rye production
	Seed cotton production
	Sesame seed production
	Sheep husbandry
	Sisal production
	Soft-Fibres production, other
	Sorghum production
	Soyabeans production
	Spices production, other
	Sugar beet production
	Sugar cane production
	Sunflower seed production
	Sweet potatoes production
	Tea production
	Tobacco production
	Tomatoes production
	Vegetable production, other
	Wheat production
	Yams production
Processing	Alcohol production, Non-Food
	Asses slaughtering
	Beer production
	Beekeeping
	Beverages production, Alcoholic
	Beverages production, Fermented
	Buffaloes slaughtering
	Camelids slaughtering, other
	Camels slaughtering
	Cattle slaughtering
	Coconut Oil extraction
	Cotton production
	Cottonseed Oil extraction
	Goats slaughtering
	Groundnut Oil extraction
	Horses slaughtering
	Maize Germ Oil extraction

Processing	Mules slaughtering Oilcrops Oil extraction, other Olive Oil extraction Palm Oil production Palmkernel Oil extraction Pigs slaughtering Poultry slaughtering Rabbits slaughtering Rape and Mustard Oil extraction Ricebran Oil extraction Rodents slaughtering, other Silkworm breeding Sesameseed Oil extraction Sheep slaughtering Soyabean Oil extraction Sugar production Sugar production, non-centrifugal Sunflowerseed Oil extraction Sweeteners production, other Wine production